

MICROCOPY RESOLUTION TEST CHART  
NATIONAL BUREAU OF STANDARDS-1963-A

0

SECURITY CLASSIFICATION OF THIS PAGE (When Data Entered)

AD-A155 152

REPORT DOCUMENTATION PAGE		READ INSTRUCTIONS BEFORE COMPLETING FORM
1. REPORT NUMBER 83-K-0535-4	2. GOVT ACCESSION NO. AD-A155152	3. RECIPIENT'S CATALOG NUMBER
4. TITLE (and Subtitle) OPTICAL PROPERTIES OF NON-CRYSTALLINE SEMICONDUCTORS	5. TYPE OF REPORT & PERIOD COVERED Interim	
	6. PERFORMING ORG. REPORT NUMBER	
AUTHOR(s) P.C. Taylor	8. CONTRACT OR GRANT NUMBER(s) N00014-83-K-0535	
PERFORMING ORGANIZATION NAME AND ADDRESS University of Utah Physics Department Salt Lake City, UT 84112	10. PROGRAM ELEMENT, PROJECT, TASK AREA & WORK UNIT NUMBERS 372-152	
7. CONTROLLING OFFICE NAME AND ADDRESS Office of Naval Research 800 N. Quincy St. Atlington, VA 22217	12. REPORT DATE 1984	
	13. NUMBER OF PAGES	
9. MONITORING AGENCY NAME & ADDRESS (if different from Controlling Office) Same as above	15. SECURITY CLASS. (of this report) Unclassified	
	15a. DECLASSIFICATION/DOWNGRADING SCHEDULE	
16. DISTRIBUTION STATEMENT (of this Report) Unlimited <div style="border: 1px solid black; padding: 5px; display: inline-block;">This document has been approved for public release and sale; its distribution is unlimited.</div>		
17. DISTRIBUTION STATEMENT (of the abstract entered in Dec. 20, if different from Report) Same as above		
18. SUPPLEMENTARY NOTES		
19. KEY WORDS (Continue on reverse side if necessary and identify by block number) Optial properties, Non-Crystalline Semiconductors, Amorphous Semiconductors, Band edge, Defects		
20. ABSTRACT (Continue on reverse side if necessary and identify by block number) (See next page.)		

DTIC  
SELECTE  
JUN 17 1985  
S A D

## 20. Abstract

The optical properties of amorphous semiconductors are dominated by the presence of a tail on the optical absorption which falls exponentially into the spectral region which is normally transparent in crystalline solids. This so-called Urbach edge is attributed to the presence of localized electronic states near the band edges in the amorphous semiconductors. A portion of this edge is shown at the high energy side of Fig. 1 where the conductivity (or the product of the index of refraction  $n$  and the absorption coefficient  $\alpha$ ) is plotted for a representative chalcogenide glass as a function of energy.<sup>1</sup> Data are shown in Fig. 1 for energies up to the band edge. A more detailed, although schematic, picture of the band edge region is shown<sup>2</sup> in Fig. 2.

Above the Urbach edge (region B in Fig. 2) the absorption remains high ( $\alpha > 10^4 \text{ cm}^{-1}$ ) due to the presence of interband electronic transitions just as those which occur in crystalline solids. Absent, however, are the singularities which are the result of the band structure in crystalline solids. Instead the amorphous semiconductors exhibit much smoother absorption spectra in the interband region. A very important question, for which a complete theoretical understanding remains elusive, is the position on the absorption edge which indicates where the major contribution changes from that due to localized to that due to extended electronic states.

Below the gap there exists an absorption "tail" (region C in Fig. 2) which in some materials can be enhanced optically by excitation with light of energy near the band gap. Several mechanisms have been identified as contributing to a tail on the absorption below the band edge. The most important contributions are probably due to specific defects such as dangling bonds, to impurity species such as  $\text{Fe}^{2+}$  and to free carrier absorption in the more highly conducting amorphous semiconductors. The below-gap absorption in the more conducting glass shown in Fig. 1 is due to the last contribution.

In addition to changes in the below-gap absorption, light at energies near the band edge can sometimes alter other optical properties of amorphous semiconductors. In particular the chalcogenide (group VI) glasses, but not the pnictide (group V) or tetrahedral (group IV) amorphous solids, exhibit a shift of the optical absorption edge and the Urbach tail to lower energies upon the application of light of energies near the band gap. This so-called photodarkening process is reversible by annealing at temperatures below the glass transition temperature. The effect has been studied in some detail but is not yet well understood. In films of chalcogenide glasses which are made under non-equilibrium conditions one can even alter the structure optically. This process is irreversible and usually consists of a photo-induced polymerization of molecules in the film.

In the chalcogenide and the pnictide amorphous semiconductors the electronic states deep in the gap are attributed to specific defects at which the lattice relaxation is strong enough in comparison to the coulomb interaction between two electrons to bind two electrons (or none) in the ground state. These so-called "negative U" centers are thought to be the only important states deep in the gap in the chalcogenide glasses. In the tetrahedrally-bonded amorphous semiconductors these negative U state are thought to be rather unimportant, and the dominant electronic state deep in the gap is attributed to a silicon dangling bond (positive U). In the group V (pnictide) amorphous solids the situation is in between those which exist in the group IV (tetrahedral) and group VI (chalcogenide) systems. For example, amorphous As and P exhibit evidence for the presence of both negative and positive U states deep in the gap.

## OPTICAL PROPERTIES OF NON-CRYSTALLINE SEMICONDUCTORS

P. Craig Taylor  
 Department of Physics  
 University of Utah  
 Salt Lake City, UT 84112

	Page
I. INTRODUCTION	2
II. MODELS	4
III. THE NATURE OF THE BAND EDGE	9
IV. PHOTODARKENING	12
V. INTERBAND TRANSITIONS	15
VI. ELECTRONIC STATES DEEP IN THE GAP	17
VII. FREE CARRIER ABSORPTION	21
VIII. SUMMARY	24
ACKNOWLEDGMENTS	25
REFERENCES	26

Justification For	
Basic RA&I	<input checked="" type="checkbox"/>
Basic TAB	<input type="checkbox"/>
Unfunded	<input type="checkbox"/>
Justification	
Date of Review: _____ Reviewer: _____ Date of Approval: _____ Approved: _____ Date of Approval: _____	
A	1

## I. INTRODUCTION

The optical properties of amorphous semiconductors are dominated by the presence of a tail on the optical absorption which falls exponentially into the spectral region which is normally transparent in crystalline solids. This so-called Urbach edge is attributed to the presence of localized electronic states near the band edges in the amorphous semiconductors. A portion of this edge is shown at the high energy side of Fig. 1 where the conductivity (or the product of the index of refraction  $n$  and the absorption coefficient  $\alpha$ ) is plotted for a representative chalcogenide glass as a function of energy.<sup>1</sup> Data are shown in Fig. 1 for energies up to the band edge. A more detailed, although schematic, picture of the band edge region is shown<sup>2</sup> in Fig. 2.

Above the Urbach edge (region B in Fig. 2) the absorption remains high ( $\alpha > 10^4 \text{ cm}^{-1}$ ) due to the presence of interband electronic transitions just as those which occur in crystalline solids. Absent, however, are the singularities which are the result of the band structure in crystalline solids. Instead the amorphous semiconductors exhibit much smoother absorption spectra in the interband region. A very important question, for which a complete theoretical understanding remains elusive, is the position on the absorption edge which indicates where the major contribution changes from that due to localized to that due to extended electronic states.

Below the gap there exists an absorption "tail" (region C in Fig. 2) which in some materials can be enhanced optically by excitation with light of energy near the band gap. Several mechanisms have been identified as contributing to a tail on the absorption below the band edge. The most important contributions are probably due to specific defects such as dangling bonds, to impurity species such as  $\text{Fe}^{2+}$  and to free carrier absorption in the more highly conducting amorphous semiconductors. The below-gap absorption in the more conducting

glass shown in Fig. 1 is due to the last contribution.

In addition to changes in the below-gap absorption, light at energies near the band edge can sometimes alter other optical properties of amorphous semiconductors. In particular the chalcogenide (group VI) glasses, but not the pnictide (group V) or tetrahedral (group IV) amorphous solids, exhibit a shift of the optical absorption edge and the Urbach tail to lower energies upon the application of light of energies near the band gap. This so-called photo-darkening process is reversible by annealing at temperatures below the glass transition temperature. The effect has been studied in some detail but is not yet well understood. In films of chalcogenide glasses which are made under non-equilibrium conditions one can even alter the structure optically. This process is irreversible and usually consists of a photo-induced polymerization of molecules in the film.

In the chalcogenide and the pnictide amorphous semiconductors the electronic states deep in the gap are attributed to specific defects at which the lattice relaxation is strong enough in comparison to the coulomb interaction between two electrons to bind two electrons (or none) in the ground state. These so-called "negative U" centers are thought to be the only important states deep in the gap in the chalcogenide glasses. In the tetrahedrally-bonded amorphous semiconductors these negative U states are thought to be rather unimportant, and the dominant electronic state deep in the gap is attributed to a silicon dangling bond (positive U). In the group V (pnictide) amorphous solids the situation is in between those which exist in the group IV (tetrahedral) and group VI (chalcogenide) systems. For example, amorphous As and P exhibit evidence for the presence of both negative and positive U states deep in the gap.

The models developed to describe localized electronic states in amorphous semiconductors were discussed in Section II. In Section III we discuss the

nature of the optical band edge in amorphous semiconductors, and in Section IV the photo-induced shift of this edge in the group VI materials. Section V presents the optical properties of amorphous semiconductors in the interband region. The nature of the electronic states deep in the gap is discussed in Section VI, and Free Carrier absorption is considered in Section VII. The last section is a summary of the most important properties.

## II. MODELS

Just as in crystalline semiconductors, there is in the amorphous semiconductors evidence for the existence of specific defects and impurities which generate localized electronic states within the band gap. Whether there exist in addition states "intrinsic" to the amorphous state, which occur as a result of the disorder, remains a matter of some debate. Near the band edge the optical absorption is dominated by an exponential dependence of the absorption coefficient  $\alpha$  on the energy. Such a functional behavior was first described by Urbach<sup>2</sup> in ionic solids. This exponential dependence is often attributed to "strained bonds"<sup>4</sup> or to induced ionization of excitons.<sup>5,6</sup>

Above the band gap the absorption is similar to that which is observed in crystalline solids but without the sharp features which are due to van Hove singularities. Phenomenological descriptions of the absorption in this region exist,<sup>7,8,9</sup> but there is no detailed microscopic picture. On the other hand, there is little reason to suspect that, apart from the singularities already mentioned, there are any major differences in the interband region between the absorption processes in crystalline and amorphous semiconductors.

It was Anderson<sup>10</sup> who first suggested that the electron-lattice relaxation in amorphous semiconductors might be sufficient to overcome the coulomb interactions between two electrons and produce electronic states which are either

doubly occupied or empty in the ground state. In the approach suggested by Anderson one considers an ensemble of localized states which are characterized by the following tight-binding Hamiltonian:

$$H = \sum_{i\sigma} E_i n_{i\sigma} + \sum_{ij\sigma} V_{ij} C_{i\sigma}^\dagger C_{j\sigma} + \sum_i U_i n_{i\uparrow} n_{i\downarrow} + \sum_{i\sigma} C_i x_i n_{i\sigma} \quad (1)$$

In Eq. (1)  $i$  and  $\sigma$  are the site and spin indices, respectively, and  $n_{i\sigma} = C_{i\sigma}^\dagger C_{i\sigma}$  is the number operator for electrons. The one electron energies, which are assumed to vary from site to site in amorphous semiconductors, are  $E_i$ . The parameters  $V_{ij}$  and  $U_i$  are hopping integrals and the coulomb repulsion between two electrons, respectively. The final term in Eq. (1) represents the electron-lattice interaction in a form first suggested by Holstein.<sup>11,12</sup> In this form the energy is assumed to be a short range, linear function of the configuration coordinates  $x_i$  with proportionality constants  $C_i$ .

The detailed solutions to Eq. (1) depend on the specific form one assumes for the phonon Hamiltonian, but it can be shown<sup>12</sup> that under fairly general conditions the highly localized states in the gap are either doubly occupied or empty. For this case the two electron excitation spectrum has no gap with states filled with two electrons up to  $E_F$  above which the states are empty. There is, of course, still a gap in the one electron spectrum which is what one measures optically. Perhaps the most attractive feature of this model is that although there are broad distributions in both individual site energies  $E_i$  and electron-lattice coupling  $C_i$ , there are no deep one-electron states and no extensive one electron band tails.

For the chalcogenide glasses several specific defect models have been proposed which are motivated by Anderson's original approach. The first such defect model (MDS model) was proposed by Mott, Davis and Street.<sup>14,15</sup> In this model the prototype amorphous solid is glassy Se or S where only chalcogen atoms

are present and each atom is bonded to two nearest neighbors via p-type wave functions. The remaining p orbital on each atom is doubly occupied but non-bonding. In this simple interpretation there is no s-p hybridization.

The defects in the MDS model are formed in pairs. If a bond is imagined to break and both electrons are trapped by one of the two chalcogen atoms which becomes negatively charged, then the remaining chalcogen is postulated to form a distorted bond with another atom on a nearby chain by utilizing the two electrons which were formerly non-bonding. This defect is positively charged and involves a three-fold coordinated atom. The singly-coordinated, negatively-charged defect is known as  $D^-$  and the triply-coordinated, positively-charged defect as  $D^+$ .

In the MDS model the formation of a  $D^+$ ,  $D^-$  pair, which need not be spatially close, from two S or Se dangling bonds ( $D^0$ ) is governed by a reaction



which is exothermic because of the strong lattice distortions (negative U). Kastner, Adler and Fritzsche<sup>16</sup> (KAF model) pointed out explicitly that the coordination of the resulting negative and positive defects was one and three, respectively, and these authors presented energetic arguments which suggested that the defects would require only a modest electron-lattice interaction for stability. In the KAF approach  $D^-$  is called  $C_1^-$  and  $D^+$ ,  $C_3^+$  in order to emphasize the coordination of the defect. These authors also clearly distinguished between those  $D^+$  and  $D^-$  defects which are separated and those which occur in close pairs.

The defects  $D^+$ ,  $D^-$  are diamagnetic in the ground state as the experimental evidence suggests.<sup>17,18</sup> Optical excitation with light near the band gap can create a metastable  $D^0$  state by removal of an electron from a  $D^-$  or by capture

of an electron at a  $D^+$ . This optically-induced paramagnetism is an important feature of the model.

There are some significant difficulties with these simple defect models for the chalcogenide glasses. The most important difficulty is the fact that more detailed calculations for glassy Se suggest that the  $D^0$  is the ground state for the system (positive  $U$ ).<sup>19</sup>

Although the MDS or KAF model is the most commonly accepted explanation for the deep gap states in the chalcogenide glasses, at least one alternative approach has been suggested. Emin<sup>20,21</sup> has suggested that the polaronic term in Eq. (1) dominates to such an extent that the observed optical properties are explained essentially by polaronic effects. Emin assumes that the width of the small polaron band is greatly increased in disordered solids over the typical values observed in crystals. If the width is on the order of the band gap,<sup>21</sup> then the electron and hole polaron bands effectively pin the Fermi energy near mid-gap as is experimentally observed.

In amorphous silicon (a-Si), hydrogenated amorphous silicon (a-Si:H) and other tetrahedrally-bonded (Group IV or III-V) amorphous alloys, the deep-gap states are thought to be paramagnetic in the ground state (a positive  $U$  system).<sup>22,23</sup> The most important deep-gap state is usually interpreted as a dangling bond on a three-coordinated silicon atom. In the best samples of a-Si:H the density of these states approaches  $\sim 10^{15}$  spins/cm<sup>3</sup>.

These deep-gap states contribute to the absorption tail in region A of Fig. 2. In region B, where the absorption depends exponentially on energy, there is a parallel with the behavior first observed by Urbach<sup>3</sup> in ionic crystals. In the ionic crystals the absorption is well represented by the following relation:

$$\alpha(\omega) \sim \exp[a(\hbar\omega - \hbar\omega_0)/kT] \quad (3)$$

where  $a$  is a constant of order unity and  $\omega_0$  is a constant which roughly corresponds to the lowest excitonic frequency. Although the amorphous semiconductors in general do not follow the temperature dependence indicated in Eq. 3, the exponential form of the edge is essentially universally observed. The slope of the edge is shallower than in crystalline insulators.

There are several explanations of the Urbach edge in amorphous semiconductors. Dow and Redfield<sup>25,26</sup> suggested that the exponential edge results from electric-microfield-induced ionization of excitons. Abe and Toyozawa<sup>24</sup> utilize Gaussian site disorder and "parabolic bands" to obtain an Urbach edge. Somewhat similar explanations have been suggested by Street et al.<sup>24</sup> and by Schweitzer and Scheffler<sup>25</sup> who explain the exponential tail in terms of "strained bonds." Finally, Cohen et al.<sup>26</sup> explain the Urbach tail in terms of transitions between localized electronic states in one band tail and extended states in the other band provided there is no strong anticorrelation between the fluctuations of the valence and conduction band edges. At present it is not entirely clear which of these approaches is the closest to being correct.

In region A of Fig. 2 the absorption is such that the imaginary part of the dielectric constant  $\epsilon''$  is proportional to  $(E - E_g)^2$  where  $E$  is the energy and  $E_g$  is a measure of the optical gap. This empirical fact was first pointed out by Tauc et al.<sup>27</sup> who used a crystalline model with disorder to explain the quadratic dependence. Other models have also reproduced this result.<sup>24,25</sup>

### III. THE NATURE OF THE BAND EDGE

Although the band edge is a reproducible, well-defined quantity in the bulk amorphous semiconductors, it can be quite variable in thin film samples. Examples of this variability in amorphous Ge and Si (a-Ge, a-Si) are shown in Figs. 3 and 4, respectively.

As shown in Fig. 3, both the position and the shape of the absorption edge are strong functions of the deposition and annealing conditions.<sup>28-31</sup> In some unannealed evaporated films of a-Ge there is a low frequency tail on the absorption which extends down to  $\sim 0.3$  eV while films deposited under other conditions exhibit much sharper edges<sup>32</sup>. Figure 3 presents a composite of various films with different absorption edges. The band edge of crystalline Ge (curve 7) is also shown for comparison. The results displayed in Fig. 3 represent films made under a variety of conditions for the substrate temperature and the annealing procedure.

At first, results such as those of Fig 3 were interpreted as evidence of tails of localized electronic states whose density was determined by some disorder parameter which was highly dependent upon deposition conditions. In fact, however, these tails in both a-Ge and a-Si are now known to be caused by defects associated with dangling bonds which are predominantly located on the internal surfaces of voids in the films. Strong signals (up to  $\sim 10^{20}$  spins  $\text{cm}^{-3}$ ) are observed in these films,<sup>33</sup> and these signals are ascribed to dangling bonds. In addition, small angle x-ray scattering<sup>34</sup> and electron diffraction<sup>35</sup> experiments have detected the presence of voids with radii as large as  $\sim 30$  Å in evaporated films of a-Ge and a-Si. The strengths of the ESR signals, the densities of voids and the density deficiencies between the films and the crystalline solids will scale with the strength of these optical absorption tails. In many cases annealing reduces all of these effects.

In a-Si typical results<sup>35</sup> are indicated in Fig. 4 for a series of films prepared under systematically varied conditions. Here also the absorption edge is observed to shift to increasingly higher energies with decreasing spin density. An extrapolation to zero spin density<sup>35</sup> yields the solid line of Fig. 4.

It is apparent from Figs. 3 and 4 that it is difficult to separate those properties of a-Si and a-Ge which are a result of the disorder and those extrinsic properties which arise from gross structural inhomogeneities such as voids. Although the optical properties of a-Si:H are much more reproducible, the same difficulty persists in this system.<sup>36</sup> Figure 5 shows the absorption edge in several well characterized films of hydrogenated amorphous silicon<sup>9</sup> (a-Si:H). In the region where  $\alpha$  is large ( $\alpha \geq 10^3 \text{ cm}^{-1}$ ) the data are taken from transmission measurements through thin films. For small  $\alpha$  ( $\alpha \leq 10^2 \text{ cm}^{-1}$ ) the data are from photoconductivity measurements which have been normalized to the absorption data. The scatter in the absorption edge is very small in this well-characterized system. The three regions shown schematically in Fig. 2 (and denoted as A, B and C) are apparent in Fig. 5.

The only significant variation from sample to sample in the a-Si:H films shown in Fig. 5 occurs in the low energy tail region (region C). Although there may be "intrinsic" processes which contribute to the absorption in this region, most of the absorption commonly observed is probably due to impurity species. A similar situation also holds in the chalcogenide glasses. Representative low energy absorption spectra are shown for three chalcogenide glasses<sup>37</sup> in Fig. 6. Bulk chalcogenide glasses also exhibit highly reproducible optical absorption edges which are relatively insensitive to preparation conditions and, under equilibrium conditions, the only observable absorption within the gap (region C) is ascribable to the presence of impurities.<sup>38</sup> The spectra of Fig. 6 were

conductivity between the d.c. and infrared frequencies (the factor  $\beta$ ). In fact, very little study has been devoted to possible free carrier absorption effects in amorphous semiconductors.

#### VIII. SUMMARY

Specific defects and impurities play a role in determining the optical properties of amorphous semiconductors just as they do in the crystalline case. Both defects and impurities give rise to absorption processes below the energy gap in many amorphous semiconductors. There are also features of the optical properties which are intrinsic to the presence of disorder, such as the Urbach tail to the absorption edge or the photodarkening of the absorption edge in group VI amorphous semiconductors.

Interband optical absorption in the amorphous semiconductors is similar to that which is observed in crystalline solids. Except for the absence of sharp features due to van Hove singularities, and features due to the selection rules such as indirect energy gaps, the spectra observed in the amorphous semiconductors are very similar to those observed in crystalline counterparts.

Electron-lattice relaxation plays an important role in determining both the defects and the intrinsic properties of the group VI amorphous semiconductors. The most important specific defects are the singly-coordinated, negatively-charged chalcogen ( $D^-$ ) and the triply-coordinated, positively-charged chalcogen ( $D^+$ ) from which one can generate neutral dangling bonds ( $D^0$ ) via optical excitation at low temperature. In the group IV amorphous semiconductors there always exist some dangling bonds in the ground state.

The absorption in amorphous semiconductors in the region of the optical energy gap has three universal and distinct features. There is a region ( $\alpha \geq 10^3 \text{ cm}^{-1}$ ) where the absorption appears to be proportional to  $E(E - E_g)^2$  where  $E_g$  defines an energy gap. This region defines the onset of interband

dependence<sup>71</sup> of the thermally activated optical absorption of  $\text{Tl}_2\text{SeAs}_2\text{Te}_3$  glass is shown for five different temperatures in Fig. 18. These data exhibit relatively little frequency dependence; the conductivity or absorption coefficient increases by about 10% as the frequency increases from 660 to 2000  $\text{cm}^{-1}$ . If it is assumed that the data are consistent with a simple Drude model for thermally generated free carriers with  $\omega\tau < 1$  ( $\omega < 10^{14}$  Hz), then for unity effective mass the observed frequency independent free carrier conductivity between 1000 and 2000  $\text{cm}^{-1}$  in  $\text{Tl}_2\text{SeAs}_2\text{Te}_3$  glass implies that the mobility is of the order of 1  $\text{cm}^2/\text{Vsec}$  at these optical frequencies. Clearly the applicability of the Drude model to this case is doubtful, but the exercise does serve to illustrate the fact that the frequency independent thermally activated absorption is consistent with very low mobility for these extended state carriers in the amorphous semiconductor.

The absorption data of Edmond<sup>72</sup> for liquid  $\text{As}_2\text{Se}_3$  in the spectral range 3000-9000  $\text{cm}^{-1}$  are also plotted in Fig. 18 for several temperatures. The optical conductivity or absorption of liquid  $\text{As}_2\text{Se}_3$  in this spectral range is thermally activated with an activation energy approximately equal to that for the d.c. conductivity of this material ( $\Delta E = 1.0$  eV). Furthermore, at 4000  $\text{cm}^{-1}$  for the highest temperatures studied the magnitude of the optical conductivity is approximately  $\beta \sim 20$  times greater than the d.c. conductivity. Obviously, the observability of optical free carrier effects is greatly enhanced in the high conductivity, narrow gap glass. Thermally activated absorption can be detected in  $\text{As}_2\text{Se}_3$  only in the molten state, while in solid  $\text{Tl}_2\text{SeAs}_2\text{Te}_3$  glass the thermally activated absorption is clearly evident between room temperature and  $T_g = 86^\circ\text{C}$ .

There exists no detailed theoretical understanding of either the frequency dependence of the free carrier absorption or the origin of the increase in the

activated carriers exists.

The chalcogenide glass  $\text{Tl}_2\text{SeAs}_2\text{Te}_3$  is one of the most highly conducting ( $\sigma_{\text{dc}}(300\text{K}) \approx 3 \times 10^{-3} \Omega^{-1} \text{cm}^{-1}$ ) bulk glass compositions known, and in this glass possible free carrier optical effects have been observed<sup>71</sup> as shown in Fig. 17. The absorption for  $\text{Tl}_2\text{SeAs}_2\text{Te}_3$  glass throughout the region below the band gap is essentially independent of frequency and strongly temperature dependent for temperatures above room temperature. The data presented in Fig. 17 demonstrate that at temperatures greater than 340K the absorption coefficient in this glass at 10 micrometers wavelength is thermally activated with a single well defined activation energy. Also shown in this figure is the temperature dependence of the d.c. conductivity in the same temperature range. There are three significant features of the data of Fig. 17: (1) the thermal activation energies for the d.c. and optical conductivities are equal within experimental error ( $\Delta E = 0.35 \text{ eV}$ ); (2) the optical conductivity in the  $660\text{-}2000 \text{ cm}^{-1}$  range is a factor  $\beta \sim 8$  larger than the d.c. conductivity; (3) there is essentially no change in the slope of either the d.c. or optical conductivity curves as the temperature passes through the softening point of the glass ( $T \approx T_g$ ).

The near equivalence of the thermal activation energies for the d.c. and optical conductivities is strong evidence that the thermally activated infrared absorption or conductivity mechanism involves thermally generated carriers in extended band states. As such, this phenomenon constitutes the nearest counterpart of a free carrier optical absorption yet observed in an amorphous semiconductor. However, the extremely low carrier mobilities which characterize amorphous semiconductors cause the frequency or wavelength dependence of this "free" carrier absorption to differ drastically from the classical plasma edge observed in crystalline semiconductors. The frequency

## VII. FREE CARRIER ABSORPTION

In chalcogenide glasses which are highly conducting ( $\sigma_{dc} \sim 10^{-3} \Omega^{-1} \text{ cm}^{-1}$ ), there exists an absorption process at energies below the band gap which is attributable to free carriers.<sup>71</sup> One chalcogenide glass which shows this effect at 300K is  $\text{Tl}_2\text{SeAs}_2\text{Te}_3$  whose absorption spectrum is shown in Fig. 1.

The effect of free carriers on the optical properties of crystalline semiconductors at wavelengths longer than those corresponding to the intrinsic absorption edge have been well characterized. Free carrier absorption observed in the infrared and far infrared in semiconductors can be described by the classical Drude treatment in terms of the carrier concentration, effective mass, and mobility or electron relaxation time. The absorption takes the form of a plasma absorption edge which increases with increasing wavelength as  $\lambda^2$ . In contrast, free carrier effects in amorphous semiconductors have not been thoroughly investigated and are not well characterized. One must keep in mind the fact that the classical  $\lambda^2$  plasma absorption edges are observed in crystalline semiconductors having electron mobilities in the range of  $10^4$ - $10^6 \text{ cm}^2/\text{Vsec}$  and carrier concentrations of the order of  $10^{17}$ - $10^{18} \text{ cm}^{-3}$ . The extremely low carrier mobilities observed in amorphous semiconductors preclude the observation of a well defined plasma edge in these materials. Furthermore, if the conductivity is related to the absorption constant by  $n\alpha(\omega) = 120 \pi\sigma(\omega)$ , where  $n$  is the refractive index,  $\alpha(\omega)$  the absorption coefficient and  $\sigma(\omega)$  the conductivity in  $\Omega^{-1} \text{ cm}^{-1}$ , it can be seen that a conductivity of at least  $10^{-1} \Omega^{-1} \text{ cm}^{-1}$  is required to produce an absorption constant  $\alpha \sim 1 \text{ cm}^{-1}$ . If we set  $\alpha \sim 1 \text{ cm}^{-1}$  as the lower limit of observability for a free carrier absorption in amorphous semiconductors, it can be seen that the observation of free carrier absorption in amorphous semiconductors is possible only for a few highly conducting compositions or at high temperatures where a high concentration of thermally

been discussed by many authors. At short times ( $\sim 10$ - $100$  nsec) after pulsed excitation some authors observe two PL peaks<sup>61,62</sup> and others one.<sup>63</sup> The time evolution of the total PL intensity is spread out over many decades in a general power law decay. In some cases<sup>64</sup> three distinct time regimes are observed. For example, in glassy  $As_2S_3$  these three regimes correspond to decays on the order of  $10^{-8}$ ,  $10^{-6}$  and  $10^{-4}$  sec. At short times it has also been observed<sup>65</sup> that the PL remains polarized parallel to the polarization of the exciting light. This polarization "memory" can exist for times up to  $\sim 10^{-4}$  sec.

There have been many conflicting results and a myriad of nuances published on the time resolved PL in the best studied chalcogenide glass,  $As_2S_3$ . The time decay suggests at least three distinct PL processes and the spectral dependence at least two. There is no universally accepted interpretation of these processes, and a coherent picture of all these effects does not yet exist.

Transient optical absorption processes have also been investigated in the chalcogenide glasses. Experiments have been performed both on nanosecond<sup>66-68</sup> and on picosecond<sup>69,70</sup> time scales. Representative results<sup>67</sup> on a nanosecond time scale for glassy  $As_2Se_3$  are shown in Fig. 16. Figure 16a shows the spectral dependence of the transient optically-induced absorption at different delay times after pulsed excitation. Figure 16b shows the temperature dependence of this absorption at a fixed delay time.

The absorption decreases and shifts to higher energies as the delay time increases (see Fig. 16a). At constant delay time, the absorption becomes less and less energy dependent as the temperature decreases (see Fig. 16b). These results have been interpreted<sup>66</sup> in terms of the trapping and subsequent thermal release of electrons and holes from localized electronic states in the band-tail region (multiple trapping model).

( $D^+$ ,  $D^-$  and  $D^0$ ) of the chalcogen defects discussed in Section II. In the small polaron model<sup>21</sup> these three experimental effects are attributed to electron-like and hole-like small polarons which can be self-trapped at arbitrary distances from one another.

In addition to the metastable ESR and optical absorption, excitation of the chalcogenide and pnictide amorphous semiconductors with light of energy near the band gap produces a metastable decrease in the PL efficiency with time.<sup>56,57</sup> This fatigued or diminished magnitude of the PL efficiency with time is shown in Fig. 15 for glassy  $As_2Se_3$  at  $\sim 10K$ . The fatigued PL does not recover if the excitation is interrupted for an arbitrary period of time, and upon resumption of excitation the PL continues to decay in intensity. After fatiguing the application of light below the gap restores the PL toward its original efficiency.

The fatiguing and restoring processes for the PL parallel the growth and decay processes, respectively, for the optically-induced ESR and absorption. Both the rates and the temperature dependences are similar for all three effects. However, these parallels do not necessarily imply that all three processes involve the same electronic states. In particular, there is good evidence to suggest that the PL fatiguing process is distinct from the other two effects.<sup>58,59</sup> The most common interpretation<sup>58,59</sup> is that the fatiguing process is due to the optical creation of a competing non-radiative channel and not directly to the defects discussed in Section II. It has also been suggested that pervasive impurities, such as Fe or Cu, may contribute to the PL fatigue.<sup>59,60</sup>

Although all of the processes discussed above involve optically-induced changes which are metastable, there are also optical effects which decay in time. In the chalcogenide glasses transient photoluminescent processes have

In the chalcogenide glasses the defect states are thought to be the diamagnetic, negative  $U$  states such as  $D^+$  and  $D^-$ . It is only upon optical excitation at low temperatures ( $\leq 200\text{K}$ ) that some of these states can be converted into metastable, deep-gap dangling bonds<sup>18</sup> ( $D^0$ ).

Under equilibrium conditions in the chalcogenide glasses the only observable absorption deep in the gap is that which we attributed to impurities in Section III. However, under optical excitation at energies near the band gap such as those which produce the optically-induced ESR,<sup>18</sup> there is a concomitant metastable increase in the absorption below the gap.<sup>18,53,54</sup> This absorption is shown for glassy  $\text{As}_2\text{S}_3$ , glassy  $\text{As}_2\text{Se}_3$  and amorphous As in Fig. 14. The absorption has an onset at an energy which is approximately one half of the energy gap and is relatively flat up to the band edge. Both the optically-induced absorption and the optically-induced ESR can be bleached by light of energy below the band gap. One can also bleach the absorption and ESR by thermal annealing at temperatures above  $\sim 200\text{K}$ . It takes very low light intensities to observe these inducing and bleaching effects ( $\sim 1\text{ mW cm}^{-2}$ ).

An analysis of the ESR spectra<sup>18</sup> shows that the metastable ESR states are not due to impurities. To the extent that one may identify the metastable absorption shown in Fig. 14 with the ESR, one may conclude that this absorption also is not due to the presence of impurities. It must be mentioned, that this conclusion, however plausible, is by no means incontrovertible.

Also shown in Fig. 14 are the rough energy ranges for the photoluminescence (PL) spectra which are always observed in these three amorphous solids. Irradiation of these solids with light near the band gap energies excites broad PL bands centered roughly at energies which are one half of the band gap energies.

In the defect models (MDS and KAF and minor modifications thereof)<sup>14-16,55</sup> the ESR, absorption and PL processes are all attributed to various charge states

conserved, one can develop a general relation for the behavior of the dielectric constant near the band edge. This relationship, which was originally suggested by Tauc,<sup>2,27,51</sup> is of the form

$$\omega^2 \epsilon''(\omega) \propto (\hbar\omega - E_g)^2 \quad (4)$$

where  $\epsilon''$  is the imaginary part of the dielectric constant ( $\epsilon = \epsilon' + i\epsilon''$ ) and  $E_g$  defines an energy gap. The optical matrix elements have been assumed to be independent of energy in the development of Eq. (4). Although the assumptions employed in deriving this equation are somewhat drastic, the predicted behavior is found in many amorphous solids.

Cody et al.<sup>52</sup> have recently suggested that the constant momentum matrix element assumed by Tauc should be replaced by a constant dipole matrix element. With this assumption the analog of Eq. (4) becomes

$$\epsilon''(\omega) \propto (\hbar\omega - E'_g)^2 \quad (5)$$

where  $E'_g$  defines an energy gap which is different from the gap defined in Eq. (4). In many a-Si:H films Eq. (5) yields a better fit<sup>52</sup> to experimental data than does Eq. (4). A representative fit is shown in Fig. 13 for an accumulation of data from 30 different films of a-Si:H. The solid line in Fig. 13 is a least squares fit to the data.

## VI. ELECTRONIC STATES DEEP IN THE GAP

In the tetrahedrally coordinated amorphous semiconductors, such as a-Si:H and related alloys, the primary state deep in the gap is thought to be a dangling bond on the group IV atom. In the best material there can be as few as  $\sim 10^{15}$  of these paramagnetic states per  $\text{cm}^3$ .

One can estimate<sup>7</sup> the number of valence electrons which contributes to each of the two peaks in the absorption spectra of Fig. 11 by applying a sum rule to a Kramers-Kronig analysis of the reflectivity data. Such calculations yield ~ 3 electrons for each of these two features. Photoemission studies indicate that there is little s-p hybridization of the bonds in  $\text{As}_2\text{S}_3$  and  $\text{As}_2\text{Se}_3$ . If this conclusion is correct, then there are approximately 3 non-bonding and 2.5 bonding electrons per atom in these two solids. Using this kind of qualitative reasoning, Drews et al.<sup>7</sup> attribute the two onsets of absorption near 2 and 8 eV in Fig. 11 to thresholds for transitions which originate from non-bonding and bonding valence band states, respectively. This qualitative description works because of the molecular nature of these solids, and the similarities between the crystalline and amorphous forms exist because the nearest neighbor bonding is virtually the same in both forms.

These same qualitative considerations are also useful in understanding the interband spectra of  $\epsilon'$  and  $\epsilon''$ , the real and imaginary parts of the dielectric constant, of a-Si:H as shown<sup>50</sup> in Fig. 12. In addition to the two differences mentioned above for the chalcogenide solids, the interband spectra for a-Si and crystalline Si also differ because crystalline silicon is an indirect gap semiconductor. This fact means that the absorption rises faster in a-Si for the region between 2 and 3 eV as shown in Fig. 12.

If one employs a sum rule to the silicon data of Fig. 12, then the data up to about 4 eV account for only 1 electron per atom in both the crystalline and amorphous phases. As in the case of the chalcogenides, the qualitative similarities are the result of similar short-range (nearest neighbor) order in the crystalline and amorphous forms.

To the extent that the electronic states in the amorphous solids can be considered as crystalline electronic states where the wave vector  $\vec{k}$  is no longer

manifestation of increased excitonic binding energies. The defect models ascribe photodarkening either to physically separated  $D^+$  and  $D^-$  defects<sup>16</sup> or to close pairs of  $D^+/D^-$  defects.<sup>15,48</sup> Tunneling modes, where chalcogen atoms can be optically excited from one metastable equilibrium position to another, have also been invoked to explain the photodarkening effect.<sup>49</sup> At present the correct explanation is elusive.

#### V. INTERBAND TRANSITIONS

The interband optical absorption of amorphous semiconductors is often similar to that observed in corresponding crystalline materials. The main differences between the crystalline and glassy spectra are the disappearance in the amorphous spectra of structure related to singularities in the crystalline densities of states and a general broadening of all features in the amorphous spectrum.

We illustrate these general trends with examples from three prototype amorphous semiconductors in Figs. 11 and 12. Figure 11 shows<sup>7,8</sup> the absorption coefficient in the approximate range from 2 to 12 eV for glassy and crystalline modifications of  $As_2S_3$  and  $As_2Se_3$ . The spectra for the layered crystalline solids are anisotropic and results are shown for the two principal lattice directions in the layer.

In both the crystals and the amorphous solids the interband absorption exhibits two peaks near 6 and 10 eV. May other chalcogenide materials show these same two features. The fact that these features are fairly universal in the crystalline and amorphous chalcogenides results from the molecular nature of most of these solids and the relatively weak influence which the presence of disorder has on the electronic densities of states.

with 1.8 eV light. The solid triangles and circles in Figs. 9 and 10 were taken on the same sample before and after photodarkening, respectively. There is thus no dramatic change in the vibrational spectrum before and after photodarkening. Measurements of  $^{75}\text{As}$  NQR under identical conditions also showed no changes. Since the NQR parameters are extremely sensitive to small changes in local bonding configurations,<sup>44</sup> one may conclude that the photodarkening processes do not involve major structural rearrangements.

In fast evaporated films of the chalcogenide glasses the application of light near band-gap energies does produce gross structural changes which are accompanied by a shift of the absorption edge to lower energies. These photostructural effects, which are both optically and thermally irreversible, should not be confused with the photodarkening processes just described. The photostructural effects are usually a photo-induced polymerization of the metastable films in which a more molecular structure is converted irreversibly into a more stable polymeric form.<sup>42,43,47</sup>

This situation is illustrated for fast evaporated films (on 300K substrates) of glassy  $\text{As}_2\text{Se}_3$  in Fig. 10b. The open squares are absorption data taken at 300K on the film as grown. The solid hexagons are data taken after irradiation at 1.8 eV, and the dashed line represents the two-phonon spectrum in bulk, glassy  $\text{As}_2\text{Se}_3$  at 300K. It is clear from this figure that the vibrational spectrum of the fast evaporated film approaches that of the bulk after optical excitation with near band-gap light.

The photostructural changes in the chalcogenide amorphous films are fairly well characterized and understood because they can be probed effectively by infrared absorption, Raman scattering and magnetic resonance spectroscopies. On the other hand, the more subtle photodarkening processes are much more difficult to interpret. In the Dow-Redfield approach the photodarkening is a

by thermal cycling to temperatures near the glass transition temperature or by optical excitation at energies below those of the band gap.<sup>43</sup>

In glassy  $\text{As}_2\text{Se}_3$  typical photodarkening effects are shown<sup>44</sup> in Fig. 9. In this figure the solid points represent data taken at 77K and the open points data at 300K. The triangles describe the band edge in the Urbach tail region (region B) for glassy  $\text{As}_2\text{Se}_3$  before the application of band gap light of any significant intensity. The circles indicate the shift of the band edge after application of light at 1.8 eV (6764 Å). It is apparent that the magnitude of the photodarkening is much greater at 77K than at 300K where there is no definitive shift of the edge for the exposure time depicted in Fig. 9. If the sample irradiated at 77K is warmed to 300K and recooled to 77K then about half of the photodarkening is annealed. Nearly all of the photodarkening can be annealed near the glass transition temperature.

The photodarkening process also occurs in at least some oxide glasses. The effect has been observed in glassy  $\text{As}_2\text{O}_3$  where apparent shifts of the band edge of several tenths of an eV are observed after irradiation with ultraviolet light.<sup>45</sup> The process does appear to require the presence of group VI elements which possess non-bonding, or lone pair, p-electrons. For example, photodarkening does not occur<sup>46</sup> in amorphous As or in the tetrahedrally coordinated amorphous solids. Neither the pnictide or tetrahedrally coordinated amorphous solids possess lone-pair p electrons.

The photodarkening processes in bulk chalcogenide glasses do not involve gross bonding changes. Measurements of infrared absorption and  $^{75}\text{As}$  nuclear quadrupole resonance (NQR) in glassy  $\text{As}_2\text{Se}_3$  suggest<sup>44</sup> that more subtle changes, which primarily involve the non-bonding electrons, are responsible for the photodarkening. As shown at the top of Fig. 10, there is essentially no change in the two-phonon infrared absorption spectrum at 77K before and after irradiation

such as Cu, Al or Ag only slightly modify the concentration of the major  $\text{Fe}^{2+}$  species and have essentially no effect on the optical absorption. Specifically, the addition of 600 ppm of Cu to the  $\text{As}_2\text{S}_3$  glass which contains 120 ppm Fe has no effect. However, Hilton, et al.<sup>41</sup> have demonstrated that a distillation procedure that removes carbon from as-received selenium greatly reduces the strength of the weak absorption tail in TI-1173 glass ( $\text{Ge}_{28}\text{Sb}_{12}\text{Se}_{60}$ ) relative to that measured by Wood and Tauc<sup>37</sup> (see Fig. 8). The mechanism for the contribution of carbon to the absorption tail undoubtedly differs from that of the Fe. Hilton et al.<sup>41</sup> also reported the presence of Fe in TI-1173 in quantities of  $\sim 1$  ppm. This contaminant could conceivably be responsible for the weak absorption tail (Fig. 8) which remains after distillation of the constituents. The difference between the optical absorption and laser calorimetry measurements on TI-1173 in Fig. 8 probably represents the effects of scattering by some inhomogeneities in the glass.

All of these measurements implicate impurities as the major source of the weak absorption tails in the chalcogenide glasses. On the basis of the experimental evidence currently available it can be safely concluded that any intrinsic contributions to the low energy tail occur at values of  $\alpha$  below  $1 \text{ cm}^{-1}$ . Comparisons with ESR measurements<sup>17,18</sup> suggest that these levels correspond to less than  $10^{16}$  intrinsic paramagnetic states per  $\text{cm}^3$ .

#### IV. PHOTODARKENING

As mentioned in Section I, all of the chalcogenide glasses exhibit a shift of the optical absorption edge to lower energies upon excitation with light of energy near the band gap.<sup>42</sup> This process, which is called photodarkening, is larger at lower temperatures and occurs faster with increasing intensity of the inducing light. The photodarkening process can be at least partially annealed

obtained by Wood and Tauc<sup>37</sup> for  $\text{As}_2\text{S}_3$  glass from Servo Corporation and for two Se-Ge alloys from Texas Instruments. These glasses were representative of the best commercially available grade of infrared transmitting, non-oxide glasses when the measurements were performed.

Concurrent measurements of magnetic susceptibility,<sup>39,40</sup>  $\chi$ , in glassy  $\text{As}_2\text{S}_3$  and  $\text{As}_2\text{Se}_3$  lead to the inescapable conclusion that the observed paramagnetism is caused by paramagnetic impurities with spin  $S$  greater than  $1/2$ . The most important impurity is  $\text{Fe}^{2+}$ . Studies of  $\text{As}_2\text{S}_3$  and  $\text{As}_2\text{Se}_3$  glasses intentionally doped with Fe show<sup>38,40</sup> that the strength of the optical absorption in the tail region C is directly proportional to the Fe content. In Fig. 7 the optical absorption curves for three  $\text{As}_2\text{S}_3$  glasses containing various amounts of Fe are compared.<sup>38</sup> The lowest curve represents nominally pure  $\text{As}_2\text{S}_3$  glass while the upper curves are for intentionally doped samples containing 26 and 120 ppm Fe (by weight). The pure  $\text{As}_2\text{S}_3$  actually contains about 5 ppm Fe.<sup>38</sup> It is difficult to obtain any chalcogenide glasses with Fe impurities on levels less than a few parts per million.

Low frequency (510 MHz) electron spin resonance (ESR) studies<sup>38</sup> of these Fe doped glasses have demonstrated that most of the Fe impurities are present in the divalent  $\text{Fe}^{2+}$  state. The combination of these ESR studies with the results of the absorption study clearly associates the low energy tail in the band edge absorption spectrum with the presence of these Fe impurities. Tauc et al.<sup>38</sup> suggest a charge transfer transition originating on the  $\text{Fe}^{2+}$  ion which yields an  $\text{Fe}^{3+}$  ion and an electron promoted to the conduction band. Such transitions involving metallic impurity ions are the dominant source of mid-gap electronic absorption in many oxide glasses.

It has also been found<sup>38</sup> that the magnetic susceptibility and absorption tail are specifically functions of Fe content, and that additions of other impurities

transitions. At lower values of  $\alpha$  the absorption is exponential in energy (Urbach region). In this regime the absorption is often interpreted as being due to transitions into localized band-tail states. At the lowest values of  $\alpha$  ( $\alpha \leq 10 \text{ cm}^{-1}$ ) there is a tail on the absorption which extends well into the band gap region. In many amorphous semiconductors this absorption tail is due to the presence of inadvertent impurities (in chalcogenides and pnictides) or to the presence of dangling bonds (in tetrahedrally coordinated amorphous semiconductors).

The application of light of energies near the band gap produces several metastable changes in the optical properties of the chalcogenide glasses. One such process, which is called photodarkening, is a shift of the absorption edge to lower energies after the application of band-gap light. A second example is the occurrence of an absorption below the gap which is metastable at low temperatures and is essentially independent of energy from the mid-gap region to the band edge. Various transient absorption changes also occur at temperatures above  $\sim 100\text{K}$ .

In highly conducting chalcogenide glasses there is evidence for free carrier absorption below the band edge. This absorption depends exponentially on the temperature (thermally activated) but is essentially independent of the energy. The energy independence is interpreted as the result of the low mobilities ( $\leq 1 \text{ cm}^2 \text{ V}^{-1} \text{ sec}^{-1}$ ) of charge carriers in the amorphous semiconductors.

#### ACKNOWLEDGMENTS

Mary Woolf and Vince Frederick are gratefully acknowledged for invaluable help with the preparation of the manuscript. Portions of the research described in this chapter were supported by the National Science Foundation under grant number DMR-83-04471 and by the Office of Naval Research.

## REFERENCES

1. Bishop, S.G., Taylor, P.C., and Mitchell, D.L., Vibrational and Free carrier optical properties of vitreous  $\text{As}_2\text{Se}_3$ , *J. Non-Cryst. Solids*, 5, 351, 1971.
2. Tauc, J., Optical properties of amorphous semiconductors, in Amorphous and Liquid Semiconductors, Tauc, J., ed., Plenum, N.Y., 1974, 159.
3. Urbach, R., Long-wavelength edge of photographic sensitivity and the electronic absorption of solids, *Phys. rev.*, 92, 1324, 1953.
4. Street, R.A., Knights, J.C., and Biegelsen, D.K., Luminescence studies of plasma-deposited hydrogenated silicon, *Phys. Rev.*, B18, 1880, 1978.
5. Dow, J.D. and Redfield, D., Electroabsorption in semiconductors: The excitonic absorption edges, *Phys. Rev. B1*, 3358, 1970.
6. Dow, J.D. and Redfield, D., Toward a unified theory of Urbach's rule and exponential absorption edges, *Phys. Rev. B5*, 594, 1972.
7. Drews, R.E., Emerald, R.L., Slade, M.L., and Zallen, R., Interband spectra of  $\text{As}_2\text{S}_3$  and  $\text{As}_2\text{Se}_3$  crystals and glasses, *Solid State Commun.*, 10, 293, 1972.
8. Zallen, R., Drews, R.E., Emerald, R.L., and Slade, M.L., *Phys. Rev. Lett.*, 26, 1564, 1971.
9. Cody, G.D., The optical absorption edge of amorphous silicon hydride ( $\text{a-Si:H}_x$ ), in Hydrogenated Amorphous Silicon, Vol. 21B, Pankove, J.I., ed., Academic Press, N.Y., 1984, 11.
10. Anderson, P.W., Model for the electronic structure of amorphous semiconductors, *Phys. Rev. Lett.*, 34, 953, 1975.
11. Holstein, T., Studies of polaron motion. I. The molecular crystal model, *Ann. Phys. (N.Y.)*, 8, 325, 1959.
12. Holstein, T., Studies of polaron motion. II. The "small" polaron, *Ann. Phys. (N.Y.)*, 8, 343, 1959.

13. Anderson, P.W., Amorphous systems in La Matière mal Condensée/Il-Condensed Matter, Balian, R. et al., eds, North Holland, Amsterdam, 1979, 161.
14. Street, R.A. and Mott, N.F., States in the gap in glassy semiconductors, *Phys. Rev. Lett*, 35, 1293, 1975.
15. Mott, N.F., Davis, E.A., and Street, R.A., States in the gap and recombination in amorphous semiconductors, *Phil. Mag.*, 32, 961, 1975.
16. Kastner, M., Adler, D., and Fritzsche, H., Valence-alternation model for localized gap states in lone-pair semiconductors, *Phys. Rev. Lett.* 37, 1504, 1976.
17. Agarwal, S.C., Nature of localized states in amorphous semiconductors--a study by electron spin resonance, *Phys. Rev.*, B7, 685, 1973.
18. Bishop, S.G., Strom, U., and Taylor, P.C., Optically induced metastable states in amorphous semiconductors, *Phys. Rev. B*15, 2278, 1977.
19. Vanderbilt, D., and Joannopoulos, J.D., Bonding coordination defect in g-Se: A "positive-U" system, *Phys. Rev. Lett.* 49, 823, 1982.
20. Emin, D., Seager, C.H., and Quinn, R.K., Small-polaron hopping motion in some chalcogenide glasses, *Phys. Rev. Lett.* 28, 813, 1972.
21. Emin, D., Phonon-assisted transition rates. I. Optical phonon-assisted hopping in solids, *Adv. Phys.* 24, 305, 1975.
22. Street, R.A., and Biegelsen, D.K., Luminescence and ESR studies of defects in hydrogenated amorphous silicon, *Solid State Commun.*, 33, 1159, 1980.
23. Street, R.A., and Biegelsen, D.K., Explanation of light induced ESR in a-Si:H; Dangling bonds with a positive correlation energy, *J. Non-Cryst. Solids*, 35 & 36, 651, 1980.
24. Abe, S., and Toyozawa, Y., Interband absorption spectra in disordered semiconductors in the coherent potential approximation, *J. Phys. Soc. Jpn.*, 50, 2185, 1981.

25. Schweitzer, L., and Scheffler, M., Electronic properties of strained bonds in amorphous silicon: The origin of the band-tail states?, AIP Conf. Proc., 120, 379, 1984.
26. Cohen, M.H., Soukoulis, C.M., and Economou, E.N., Interband optical absorption in amorphous semiconductors, AIP Conf. Proc., 120, 371, 1984.
27. Tauc, J., Grigorovici, R., and Vancu, A., Optical properties and electronic structure of amorphous germanium, Phys. Status Solidi, 15, 627, 1966.
28. Clark, A.H., Electrical and Optical Properties of Amorphous Germanium, Phys. Rev., 154, 750, 1967.
29. Theye, M.L., Influence of deposition conditions on the properties of amorphous germanium films, Opt. Commun., 2, 329, 1970.
30. Connell, G.A.N., and Paul, W., Is there an intimate relationship between amorphous and crystalline semiconductors?, J. Non-Cryst. Solids, 8-10, 215, 1972.
31. Temkin, R.J., Connell, G.A.N., and Paul, W., Variation of the structural and optical properties of amorphous germanium with substrate temperature, in Proc. 5th Int. Conf. on Amorphous and Liquid Semiconductors, Stuke, J., and Brenig, W., eds., Taylor and Francis, London, 1974, 133.
32. Brodsky, M.A., and Title, R.S., Electron spin resonance in amorphous silicon, germanium, and silicon carbide, Phys. Rev. Lett. 23, 581, 1969.
33. Shevchik, N.J. and Paul, W., The structure of amorphous Ge, J. Non-Cryst. Solids, 8-10, 381, 1972.
34. Moss, S.C., and Graczyk, J.F., Evidence of voids within the as-deposited structure of glassy silicon, Phys. Rev. Lett. 23, 1167, 1969.
35. Brodsky, M.H., Kaplan, D.M., and Ziegler, J.F., Optical absorption of amorphous silicon as a function of decreasing spin concentrations, in Proc. 11th Int. Conf. on the Physics of Semiconductors, Miasek, M., ed.,

- Polish Scientific Publishers, Warsaw, 1972, 529.
36. Cody, G.D., Tiedge, T., Abeles, B., Brooks, B., and Goldstein, Y., Disorder and the optical absorption edge of hydrogenated amorphous silicon, *Phys. Rev. Lett.*, 47, 1480, 1981.
  37. Wood, D.L., and Tauc, J., Weak absorption tails in amorphous semiconductors, *Phys. Rev.*, B5, 3144, 1972.
  38. Tauc, J., DiSalvo, F.J., Peterson, G.E., and Wood, D.L., Magnetic susceptibility of chalcogenide glasses, in Amorphous Magnetism, Hooper, H.O., and de Graaf, A.M., eds., Plenum, N.Y., 1973, 119.
  39. DiSalvo, F.J., Menthe, A., Waszczak, J.V. and Tauc, J., Magnetic susceptibility of amorphous semiconductors, *Phys. Rev.* B6, 4574, 1972.
  40. Gubser, D.U., and Taylor, P.C., Low temperature magnetic susceptibility of vitreous  $As_2Se_3$ , *Phys. Lett.*, 40A, 3, 1972.
  41. Hilton, A.R., Hayes, D.J., and Rechtin, M.D., Chalcogenide glasses for high energy laser applications, T.I. Technical Reports 08-74-06 and 08-74-44, Texas Instruments, 1974, unpublished.
  42. de Neufville, J.P., Photostructural transformations in amorphous solids, in Optical Properties of Solids--New Developments, Seraphin, B.O., ed., North Holland, Amsterdam, 1976, 437.
  43. Tanaka, K., Reversible photo-induced structural changes in chalcogenide glasses, *AIP Conf. Proc.*, 31, 148, 1976.
  44. Treacy, D.J., Taylor, P.C., and Klein, P.B., Photodarkening and photostructural effects in glassy  $As_2Se_3$ , *Solid State Commun.*, 32, 423, 1979.
  45. Pontuschka, W.M., and Taylor, P.C., ESR in x-irradiated  $As_2O_3$  glass, *Solid State Commun.*, 38, 573, 1981.

46. Mytilineau, E., Taylor, P.C., and Davis, E.A., On the absence of photo-darkening in pnictide amorphous semiconductors, *Solid State Commun.* 35, 497, 1980.
47. Tanaka, K., and Kikuchi, M., Anomalous photo-induced shift of optical transmission edge observed in amorphous  $As_2S_3$  film, *Solid State Commun.*, 11, 1311, 1972.
48. Biegelsen, D.K., and Street, R.A., Photoinduced defects in chalcogenide glasses, *Phys. Rev. Lett.*, 44, 803, 1980.
49. Tanaka, K., Photo-induced dynamical changes in amorphous  $As_2S_3$  films, *Solid State Commun.*, 34, 201, 1980.
50. Bagley, B.G., Aspnes, D.E., Celler, G.K., and Adams, A.C., Optical characterization of chemically vapor deposited and laser-annealed polysilicon, in Laser and Electron Beam Interactions with Solids, Appleton, B.R., and Celler, G.K., eds., Elsevier, Amsterdam, 1982, 483.
51. Tauc, J., Optical properties and electronic structure of amorphous semiconductors, in Optical Properties of Solids, Nudelman, S., and Mitra, S.S., eds., Plenum, N.Y., 1969, 123.
52. Cody, G.D., Brooks, B.G., and Abeles, B., Optical absorption above the optical gap of amorphous silicon hydride, *Solar Energy Mat.*, 8, 231, 1982.
53. Bishop, S.G., Strom, U., and Guenzer, C.S., Optical enhancement and excitation spectra of photoluminescence in chalcogenide glasses, in Amorphous and Liquid Semiconductors, Stuke, J., and Brenig, W., eds., Taylor and Francis, London, 1974, 963.
54. Cernogora, J., Mollot, F., and Benoit á la Guillaume, C., Variation of the absorption coefficient after optical excitation in arsenic III selenide at 1.6K, in Proc. Int. Conf. on The Physics of Semiconductors, 12th, Pilkuhn, M.H., ed., Teubner, Stuttgart, 1974, 1027.

55. Kastner, M., and Fritzsche, H., Defect chemistry of lone-pair semiconductors, *Philos. Mag.*, B37, 199, 1978.
56. Cernogora, J., Mollot, F., and Benoit à la Guillaume, C., Radiative recombination in amorphous  $As_2Se_3$ , *Phys. Stat. Solidi*, A15, 401, 1973.
57. Street, R.A., Searl, T.M., and Austin, I.G., Photoluminescence in amorphous  $As_2S_3$ , *J. Phys.*, C6, 1830, 1973.
58. Kastner, M., and Hudgens, S.J., Evidence for the neutrality of luminescence centers in chalcogenide glasses, *Philos. Mag.*, 37, 665, 1978.
59. Bishop, S.G., and Taylor, P.C., Iron impurities as non-radiative recombination centers in chalcogenide glasses, *Philos. Mag.*, B40, 483, 1979.
60. Bishop, S.G., Shanabrook, B.V., Strom, U., and Taylor, P.C., Comparison of optically induced localized states in chalcogenide glasses and their crystalline counterparts, *J. de Phys.* 42, C4-383, 1981.
61. Murayama, K., Ninomiya, T., Suzuki, H., and Morigaki, K., Luminescence with short decay time in arsenic chalcogenide glasses, *Solid State Commun.*, 24, 197, 1977.
62. Bösch, M.A., and Shah, J., Time-resolved photoluminescence spectroscopy in amorphous  $As_2S_3$ , *Phys. Rev. Lett.*, 42, 118, 1979.
63. Higashi, G.S. and Kastner, M., Time resolved spectroscopy of valence-alternation-pair luminescence in  $a-As_2S_3$ , *J. Non-Cryst. Solids*, 35 & 36, 921, 1980.
64. Murayama, K., and Ninomiya, T., Photoluminescence decay in amorphous  $As_2S_3$ , *Jpn. J. Appl. Phys.*, 21, L512, 1982.
65. Murayama, K., Kimura, K., and Ninomiya, T., Time dependence of the polarization of the luminescence in chalcogenide glasses, *Solid State Commun.*, 36, 349, 1980.

66. Orenstein, J. and Kastner, M., Time-resolved optical absorption and mobility of localized charge carriers in a-As<sub>2</sub>Se<sub>3</sub>, Phys. Rev. Lett., 43, 161, 1979.
67. Orenstein, J., and Kastner, M., Photocurrent Transient Spectroscopy: measurement of the density of localized states in a-As<sub>2</sub>Se<sub>3</sub>, Phys. Rev. Lett., 46, 1421, 1981.
68. Orenstein, J., Kastner, M.A., and Vaninov, V., Transient photoconductivity and photo-induced absorption in amorphous semiconductors, Philos. Mag., B46, 23, 1982.
69. Fork, R.L., Shank, C.V., Glass, A.M., Migus, A., Bösch, M.A., and Shah, J., Picosecond dynamics of optically induced absorption in the band gap of As<sub>2</sub>S<sub>3</sub>, Phys. Rev. Lett., 43, 394, 1979.
70. Ackley, D.E., Tauc, J., and Paul, W., Picosecond relaxation of optically induced absorption in amorphous semiconductors, Phys. Rev. Lett., 43, 715, 1979.
71. Mitchell, D.L., Taylor, P.C., and Bishop, S.G., Free-carrier optical absorption in vitreous Tl<sub>2</sub>SeAs<sub>2</sub>Te<sub>3</sub>, Solid State Commun., 9, 1833, 1971.
72. Edmond, J.T., Electronic conduction in As<sub>2</sub>Se<sub>3</sub>, As<sub>2</sub>Se<sub>2</sub>Te and similar materials, Br. J. Appl. Phys., 17, 979, 1966.

## FIGURE CAPTIONS

- Fig. 1. Room temperature conductivity (or absorption coefficient times index of refraction) of glassy  $\text{Tl}_2\text{Se}.\text{As}_2\text{Te}_3$  as a function of wavenumber on a log-log scale. Circles designate experimental data. From  $10^9$  to  $10^{11}$  Hz the data are from dielectric loss experiments. The data from  $10^{11}$  to  $10^{14}$  Hz result from reflectivity and transmission measurements. The dashed curve represents the contribution to the phonon absorption spectrum which is thought to be due to the presence of anharmonic tunneling modes at low energies. (After ref. 1).
- Fig. 2. Schematic diagram of a typical absorption edge in an amorphous semiconductor showing the onset of interband transitions (A), the Urbach tail (B) and the residual below gap absorption (C) (after ref. 2).
- Fig. 3. Absorption coefficient of amorphous and crystalline Ge as a function of energy from 0.3 to 1.4 eV. The substrate temperature for deposition  $T_S$  is a parameter. (1) Sputtered film,  $T_S = 25^\circ\text{C}$ , (2) sputtered film,  $T_S = 350^\circ\text{C}$ , (3) sputtered film,  $T_S = 25^\circ\text{C}$  with annealing of  $150^\circ\text{C}$  for 100 hours, (4) evaporated film,  $T_S = 25^\circ\text{C}$ , (5) evaporated film,  $T_S = 25^\circ\text{C}$  with annealing at  $300^\circ\text{C}$ , (6) evaporated film  $T_S = 300^\circ\text{C}$ , (7) crystalline Ge (after ref. 31).
- Fig. 4. Absorption coefficient as a function of energy for three representative films of amorphous Si with varying densities of unpaired spins in the gap  $N_S$ . The solid curve is an extrapolated spectrum for  $N_S = 0$  (after ref. 36).

- Fig 5. Optical absorption coefficient determined by transmission (solid points) and photoconductivity (open points) in a-Si:H films at 300K. (After ref. 36).
- Fig. 6. Optical absorption coefficient as a function of energy for three semiconducting glasses at 300K (after ref. 37).
- Fig. 7. Optical absorption coefficient as a function of energy for nominally pure and Fe-doped  $\text{As}_2\text{Se}_3$  glass at 300K (after ref. 38).
- Fig. 8. Optical absorption coefficient as a function of energy for  $\text{Ge}_{28}\text{Sb}_{12}\text{Se}_{60}$  glass (TI-1173) at 300K. (a) Relatively impure sample (Tauc et al., ref. 37; Fig. 6 of this chapter), (b) purified sample measured by standard transmission techniques, and (c) purified sample measured by calorimetric techniques (after ref. 41).
- Fig. 9. The absorption coefficient of bulk glassy  $\text{As}_2\text{Se}_3$  as a function of energy in the region of the electronic band edge. The open circles refer to measurements at room temperature and the solid symbols to measurements at 77K. Triangles represent as-received samples; circles represent samples irradiated at 6764 Å, solid squares represent samples irradiated, warmed to 300K and cooled to 77K for measurement (after ref. 44).
- Fig. 10. The absorption of glassy  $\text{As}_2\text{Se}_3$  as a function of wavenumber in the two-phonon region. (a) Bulk  $\text{As}_2\text{Se}_3$  (500  $\mu\text{m}$  thick) at 77K. Triangles represent as-received samples and circles represent samples irradiated at 6764 Å, (b) thin film of  $\text{As}_2\text{Se}_3$  (150  $\mu\text{m}$  thick) deposited on a 300K substrate and measured at 300K. Squares represent as-received samples and hexagons represent samples irradiated at 6764 Å. The dashed line represents the data of the bulk sample at 300K (after ref. 44).

- Fig. 11. Interband optical absorption coefficient for glassy (dashed lines) and crystalline (solid lines)  $\text{As}_2\text{Se}_3$  and  $\text{As}_2\text{S}_3$  at 300K. (After ref. 8).
- Fig. 12. The real and imaginary parts of the dielectric constant ( $\epsilon_1$  and  $\epsilon_2$ , respectively) for crystalline and amorphous silicon. The amorphous silicon samples were made by low pressure CVD at a substrate temperature of 625°C. (After ref. 50).
- Fig. 13. The imaginary part of the dielectric constant  $\epsilon_2$  plotted as  $\epsilon_2^{1/2}$  as a function of energy in films of a-Si:H. The solid line is a least squares fit to the data between 1.65 and 3.00 eV. (After ref. 52).
- Fig. 14. Optically induced absorption spectra for glassy  $\text{As}_2\text{Se}_3$ ,  $\text{As}_2\text{S}_3$  and amorphous As at  $\sim 6\text{K}$ . The approximate ranges for the PL bands are also indicated. (After ref. 18).
- Fig. 15. Time decay of total photoluminescence intensity in glassy  $\text{As}_2\text{Se}_3$  at  $\sim 10\text{K}$ . The intensity of the exciting light is a factor of two greater for curve (a) than for curve (b) (after ref. 56).
- Fig. 16. Photo-induced absorption below the band gap in glassy  $\text{As}_2\text{Se}_3$  (a) at  $\sim 300\text{K}$  for several delay times after pulsed excitation for  $\sim 10$  nsec. The spectra at  $10^{-4}$ ,  $10^{-3}$  and  $10^{-2}$  sec have been normalized by factors of 1.6, 2.7 and 9.3, respectively. The maximum absorption at  $10^{-5}$  sec is  $\sim 1 \text{ cm}^{-1}$ . (b) photo-induced absorption at a fixed delay time ( $10^{-3}$  sec) for various temperatures (after ref. 67).
- Fig. 17. The conductivity at d.c. and optical (infrared) frequencies as a function of reciprocal temperature in glassy and liquid  $\text{Tl}_2\text{SeAs}_2\text{Te}_3$ . The open triangles, circles, crosses, and diamonds represent data taken at 2,000, 1,000, 666 and 200-300  $\text{cm}^{-1}$ , respectively. The

solid triangles represent d.c. measurements. The glass transition temperature  $T_g$  is  $80^\circ\text{C}$  for this material. The slope of the two solid lines corresponds to an activation energy  $\Delta E = 0.35 \text{ eV}$ . Sample thickness varied from 25 to  $860 \mu\text{m}$  (after ref. 71).

Fig. 18. Frequency dependence of the thermally activated conductivity in glassy  $\text{Tl}_2\text{SeAs}_2\text{Te}_3$  and in glassy and liquid  $\text{As}_2\text{Se}_3$  (after ref. 71).

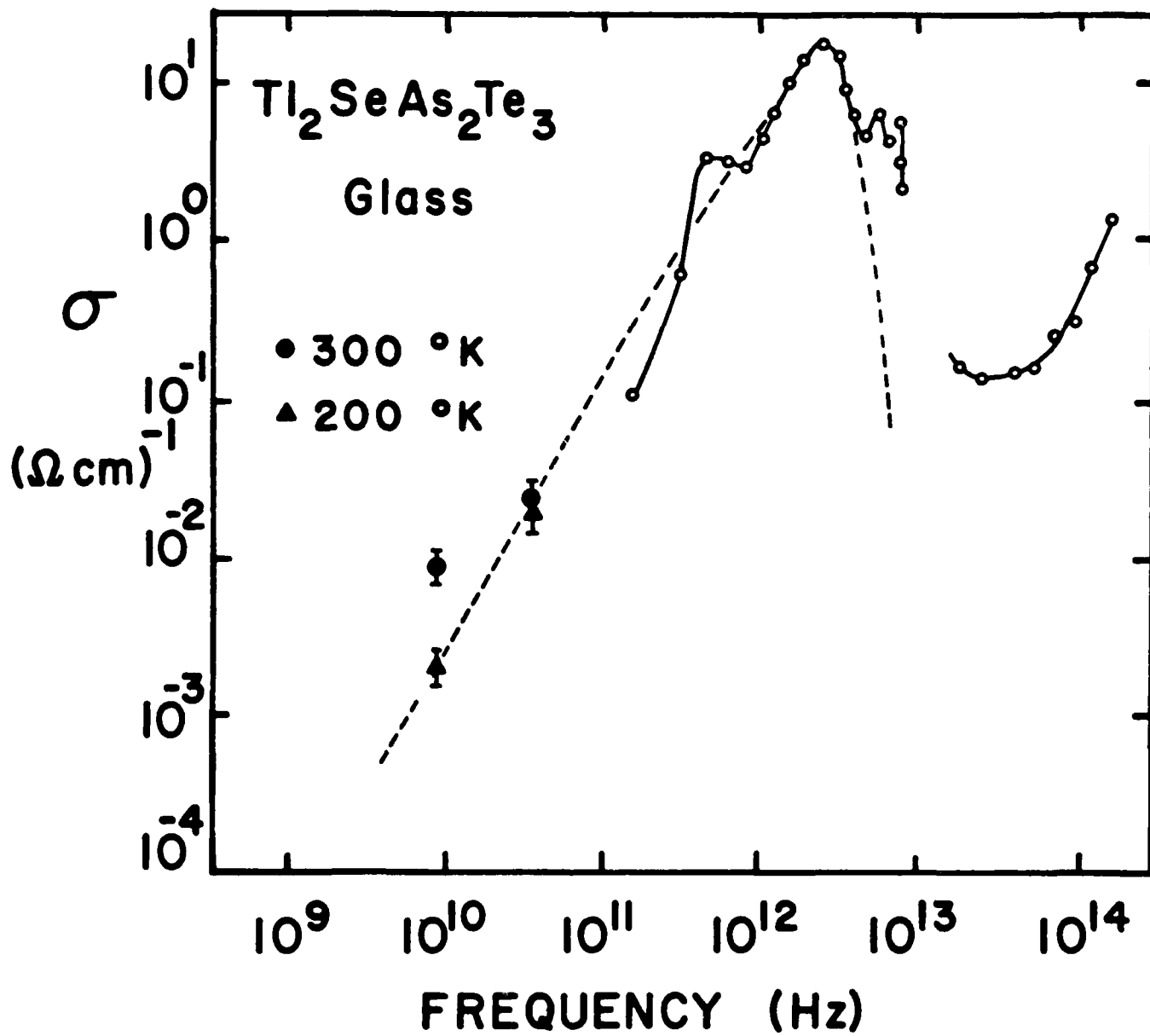


Fig. 1

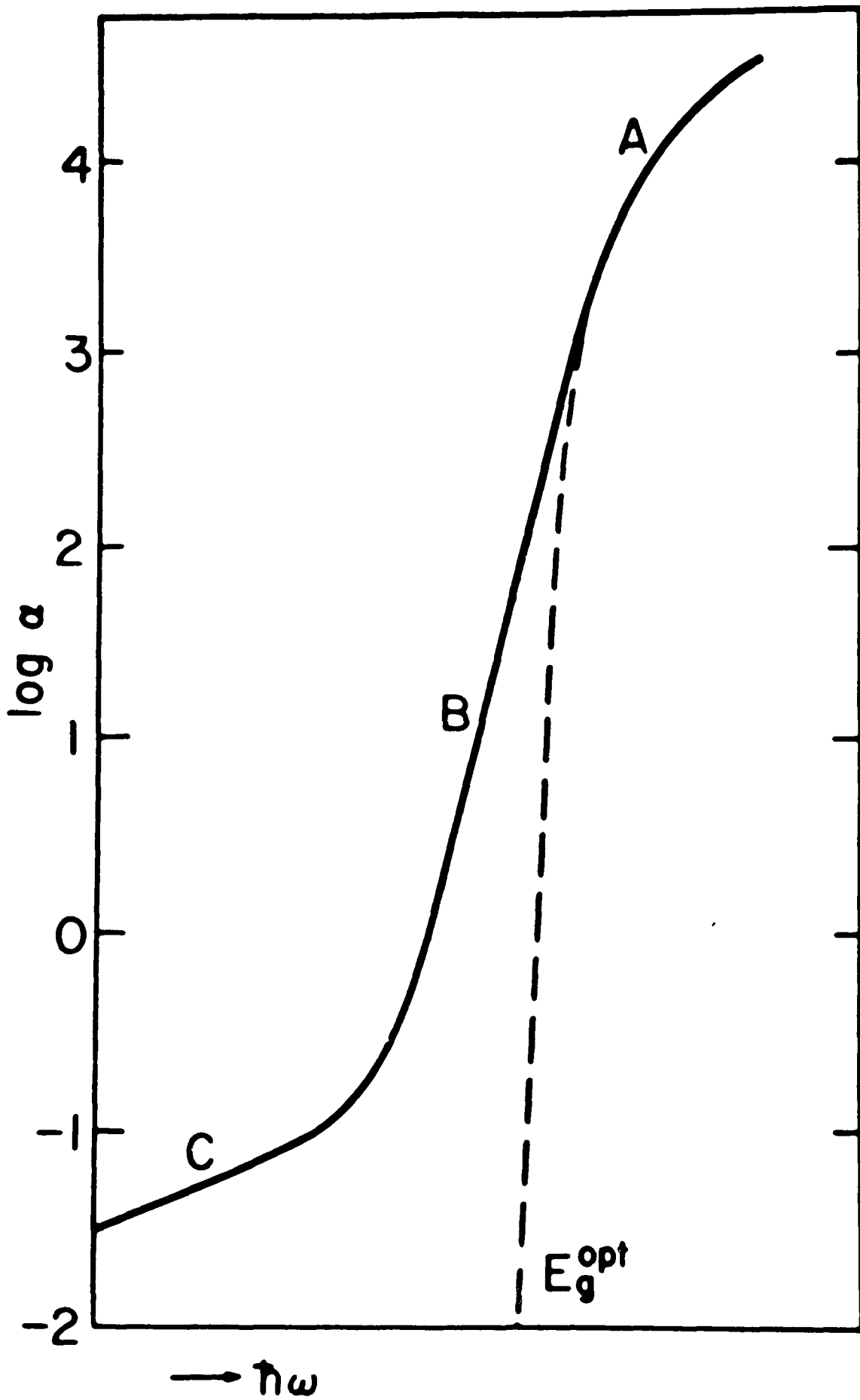


Fig. 2

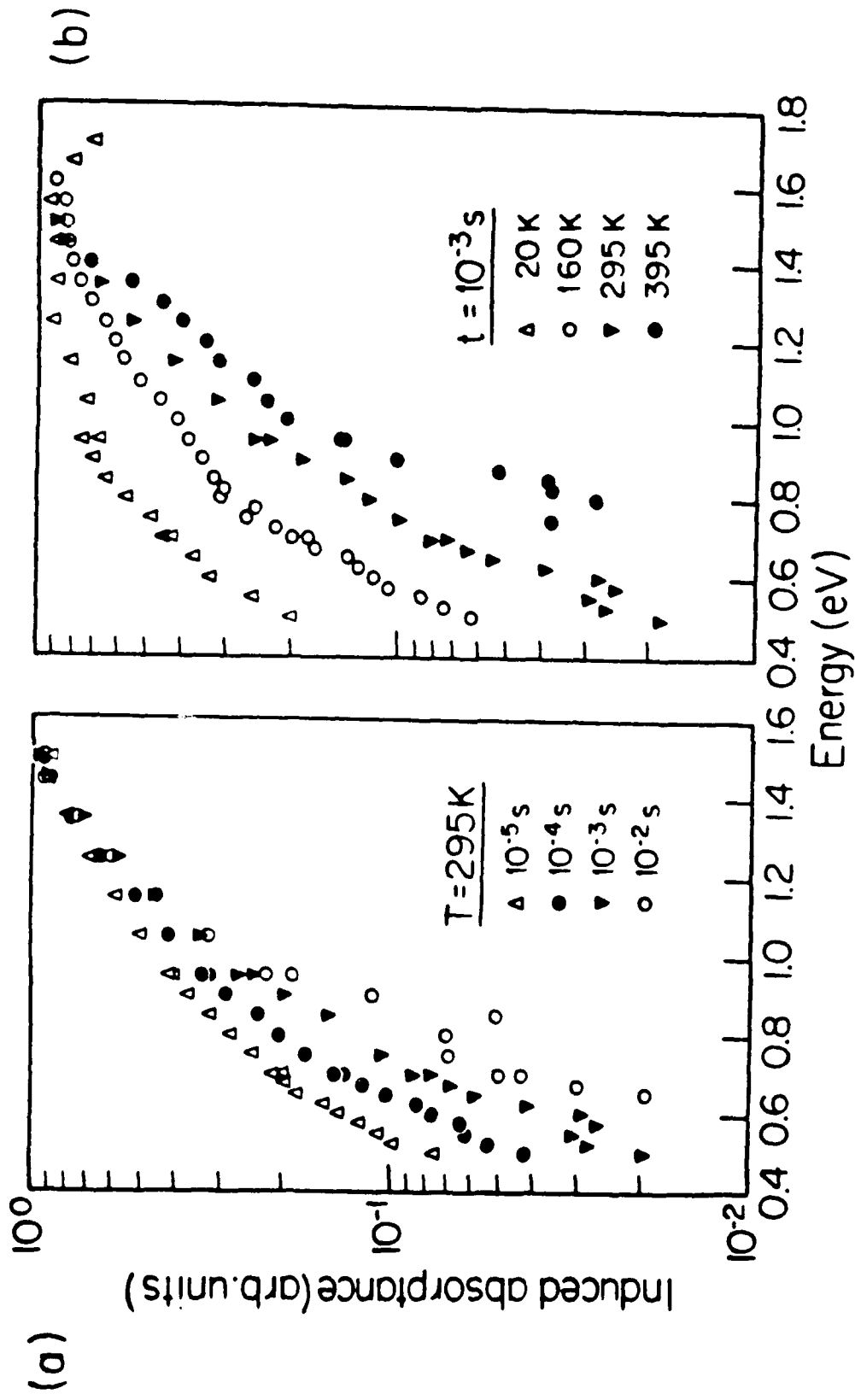


Fig. 16

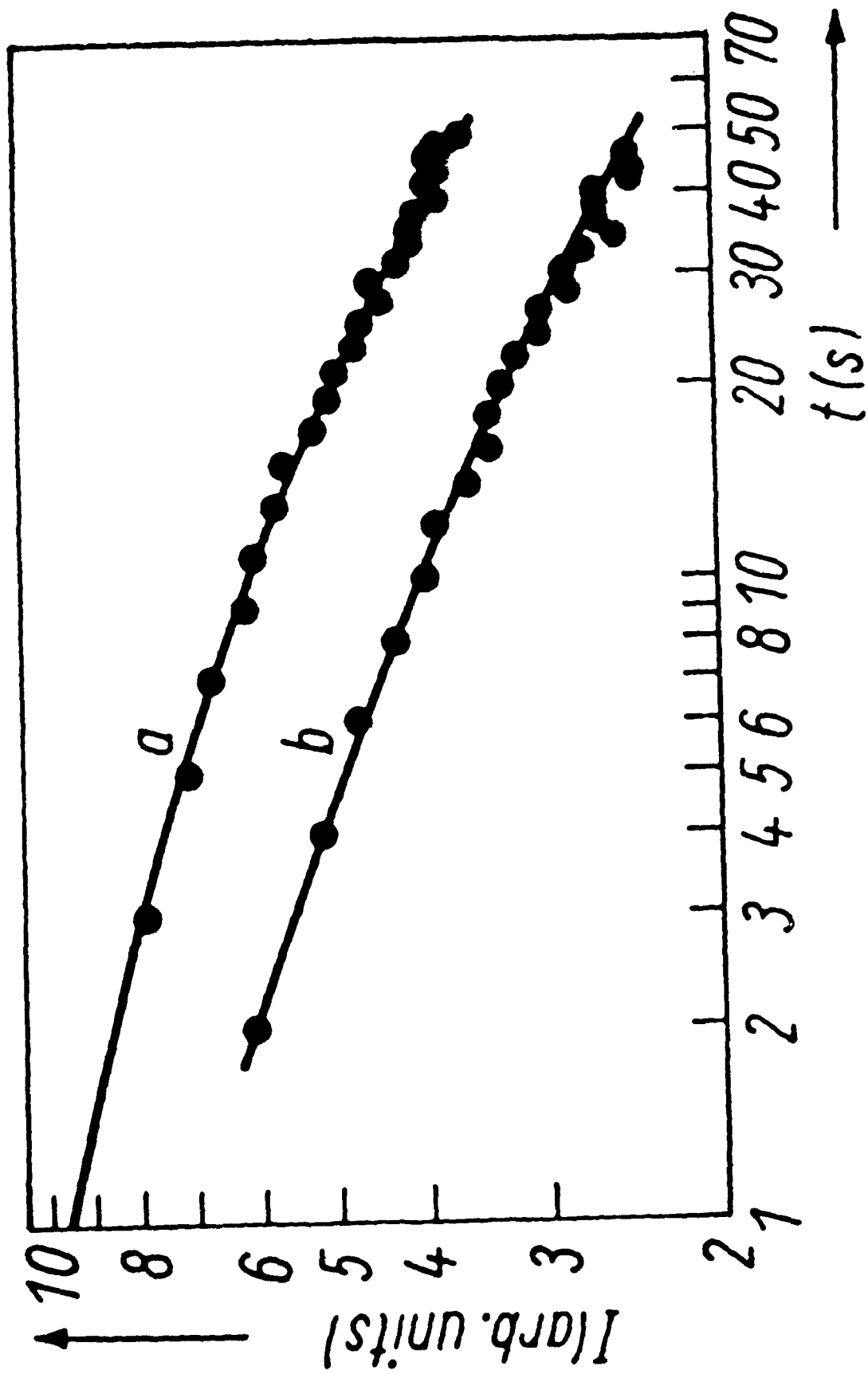


Fig. 15

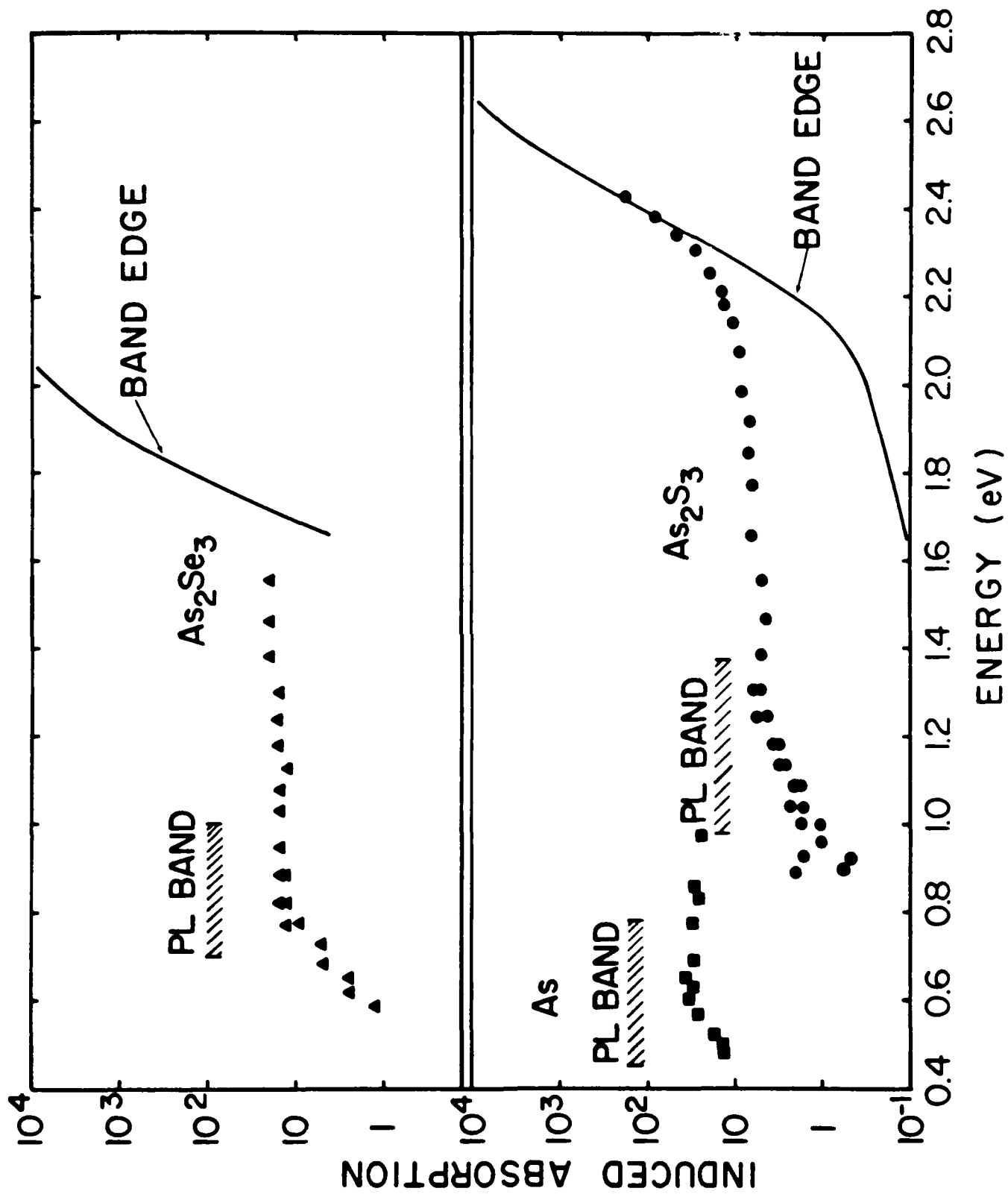


Fig. 14

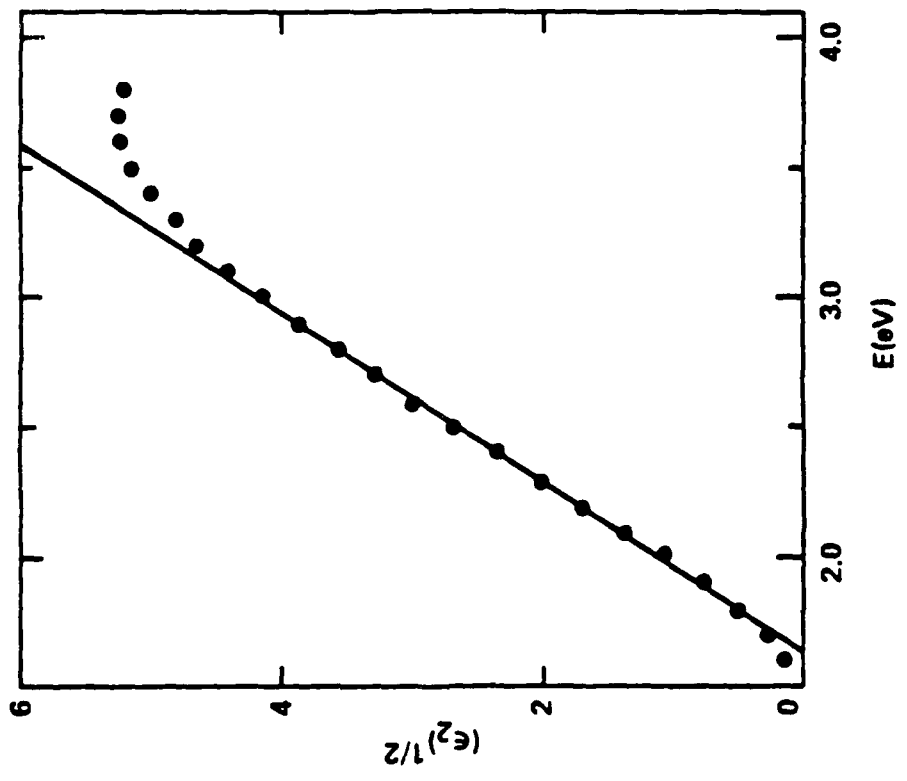


Fig. 13

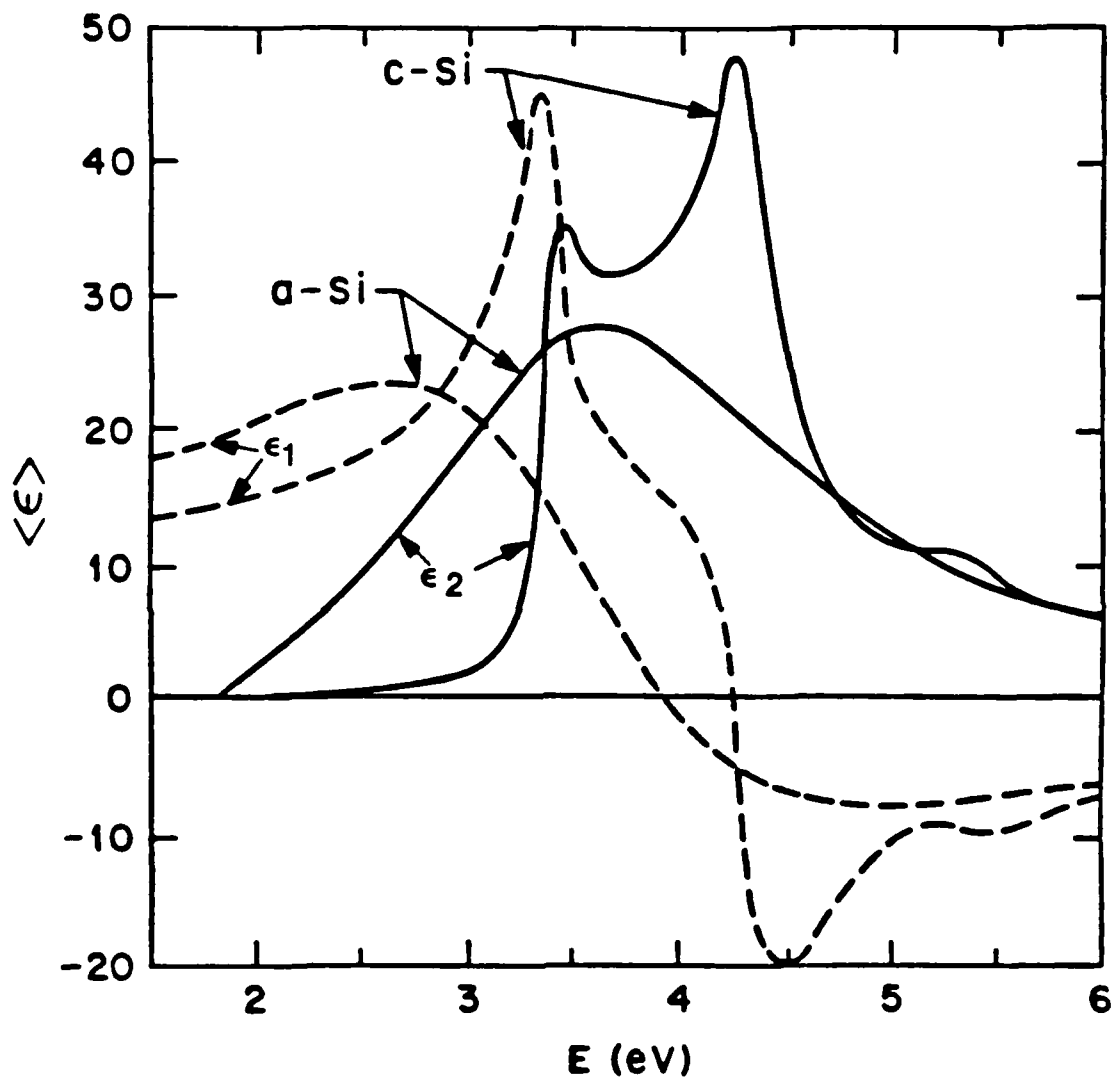


Fig. 12

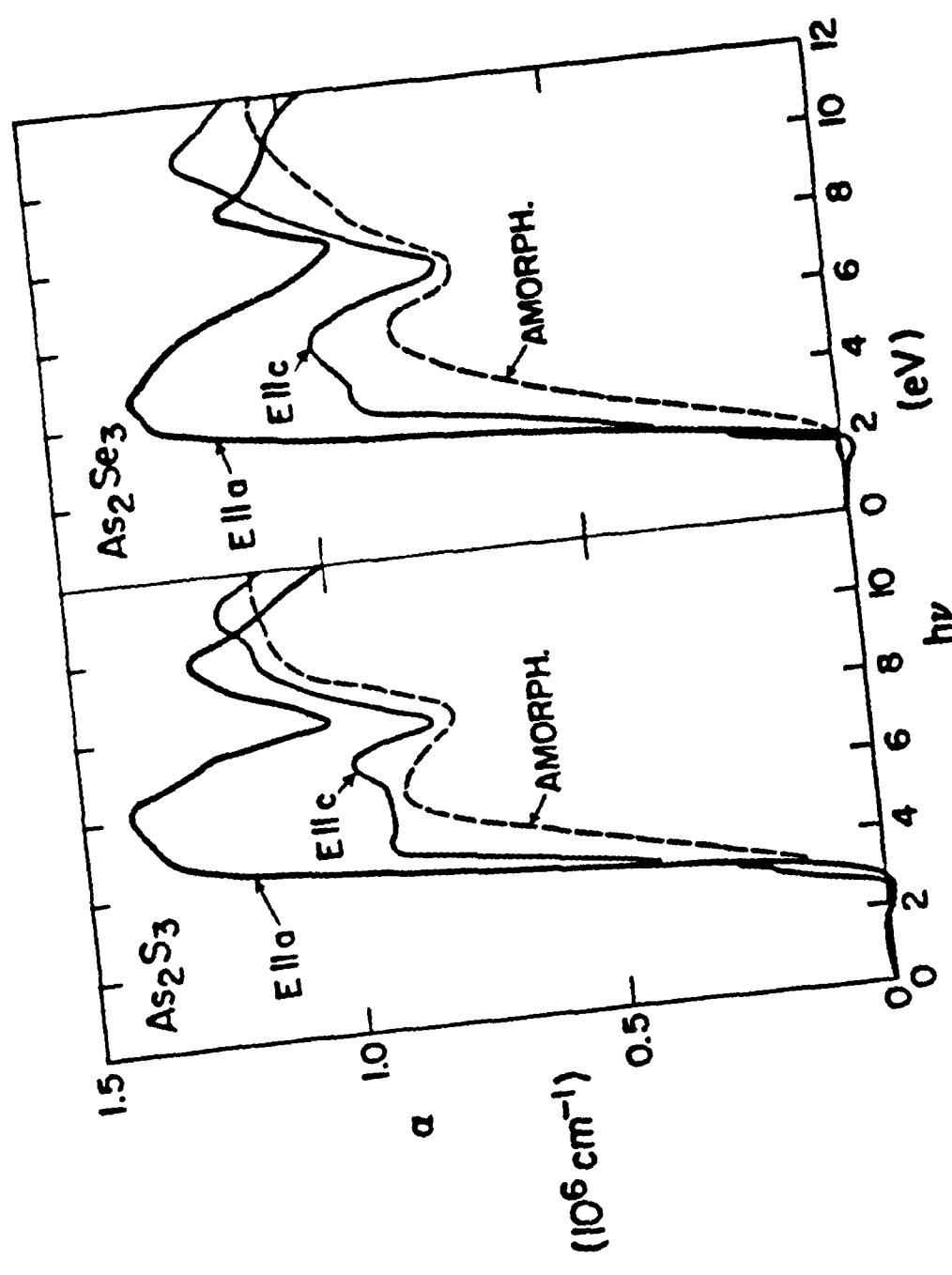


Fig. 11

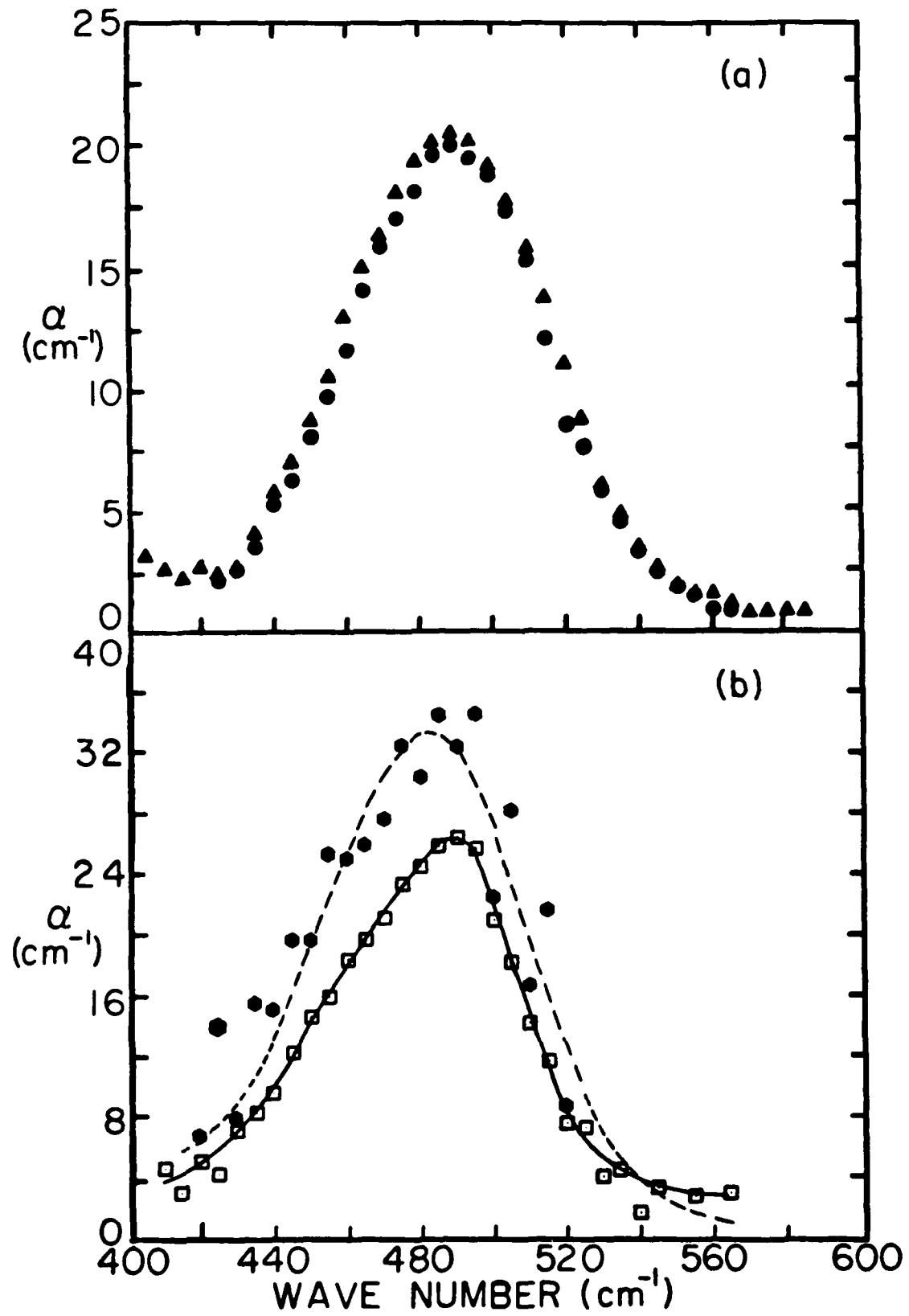


Fig. 10

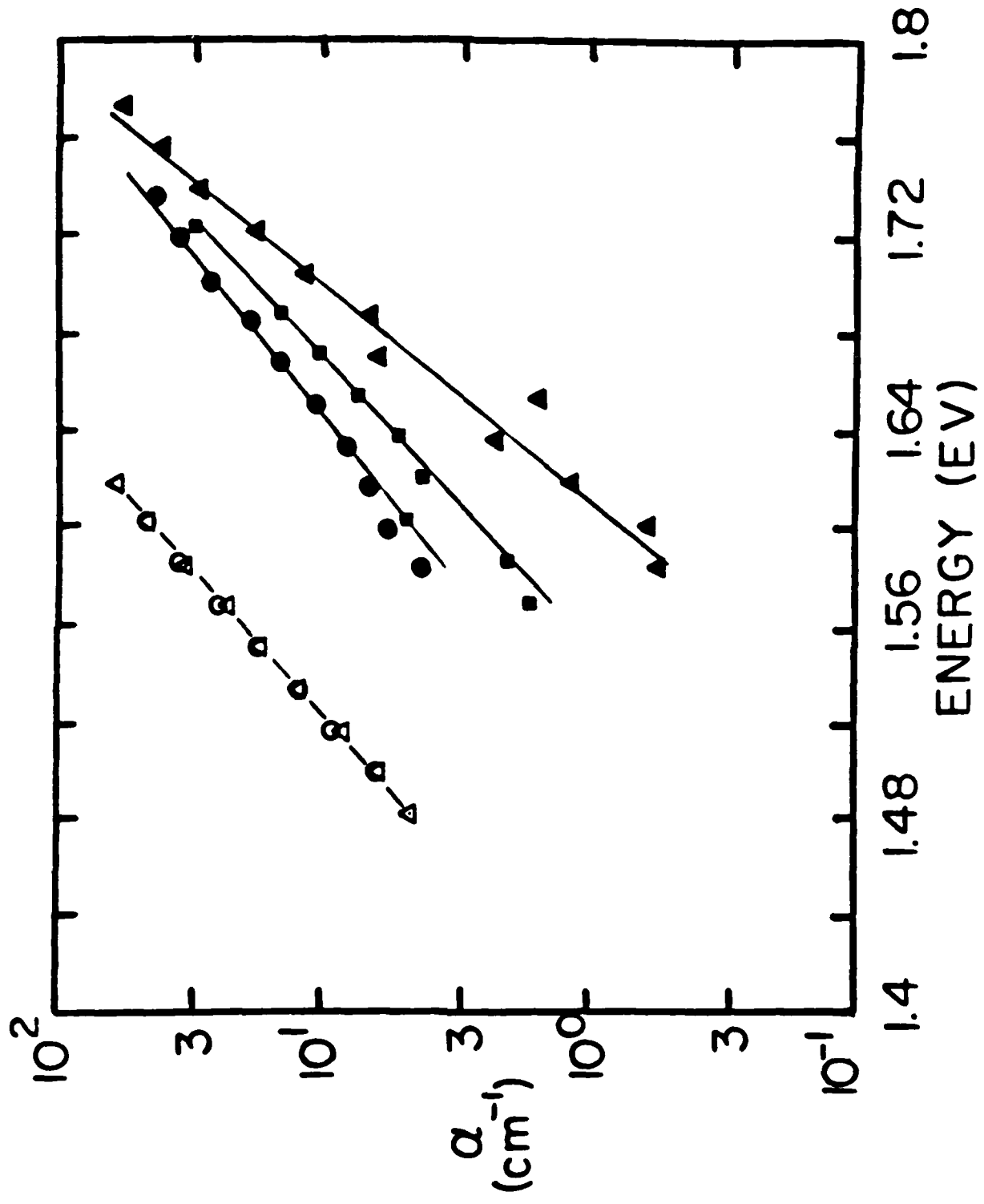


Fig. 9

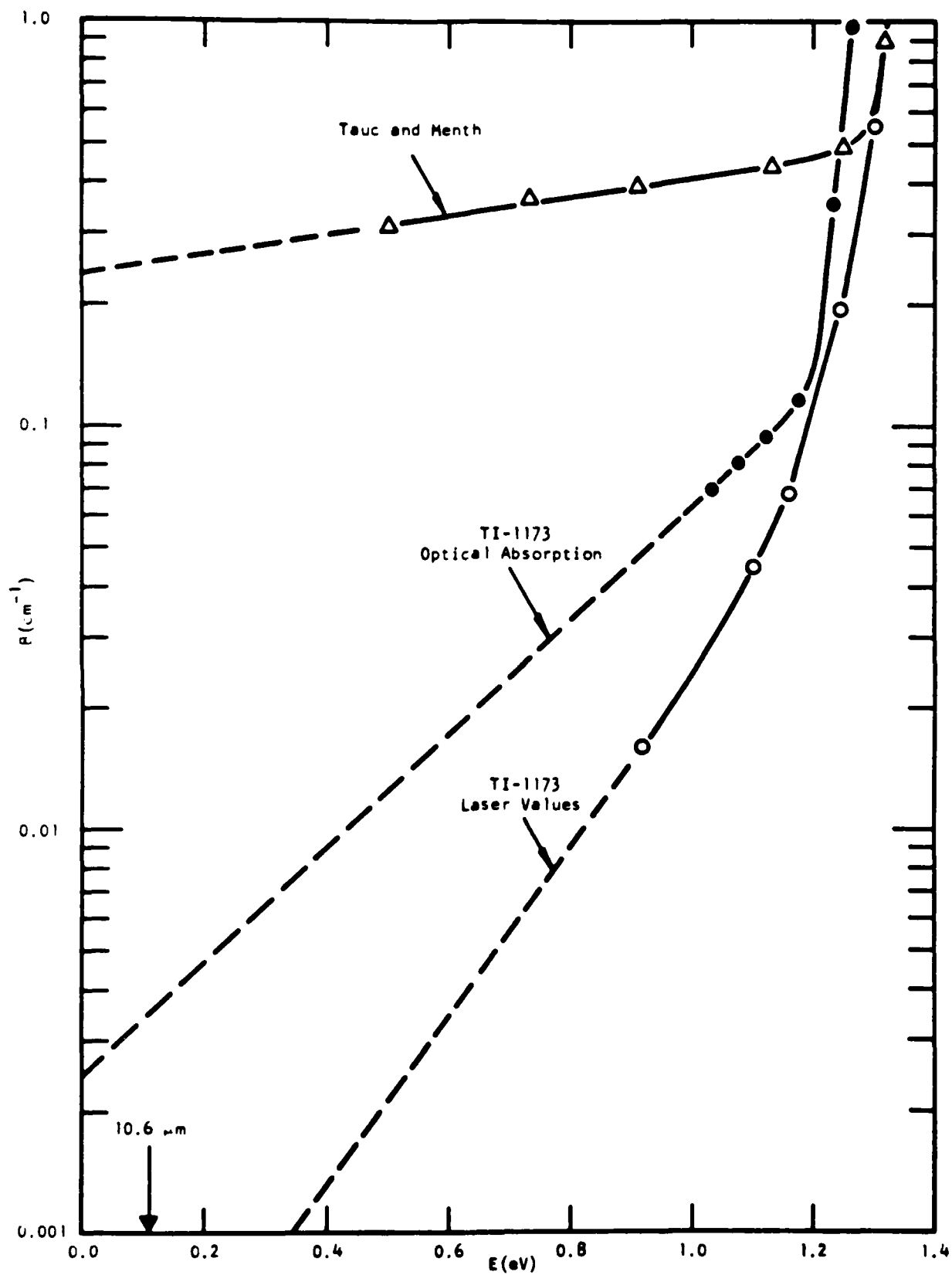


Fig. 8

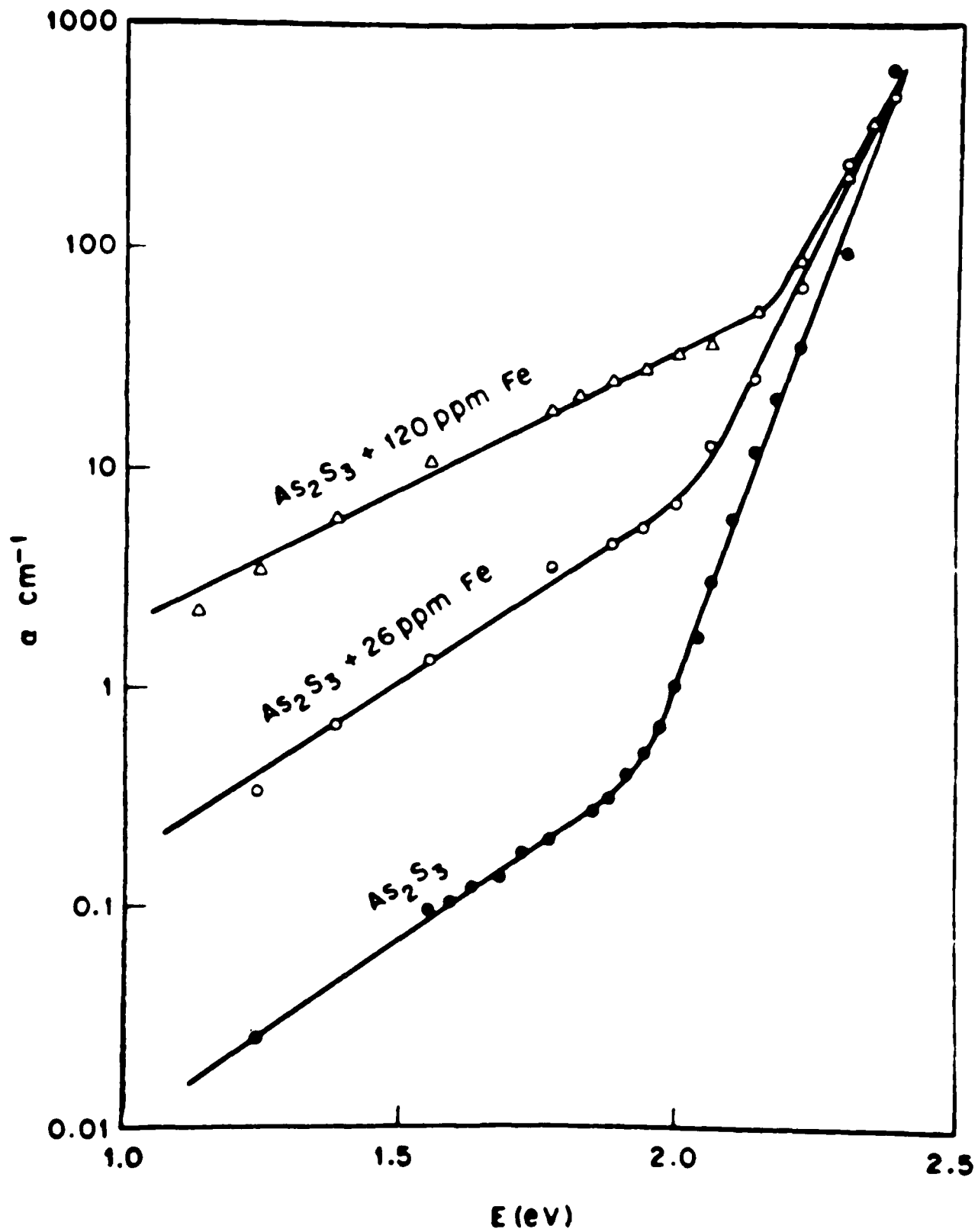


Fig. 7

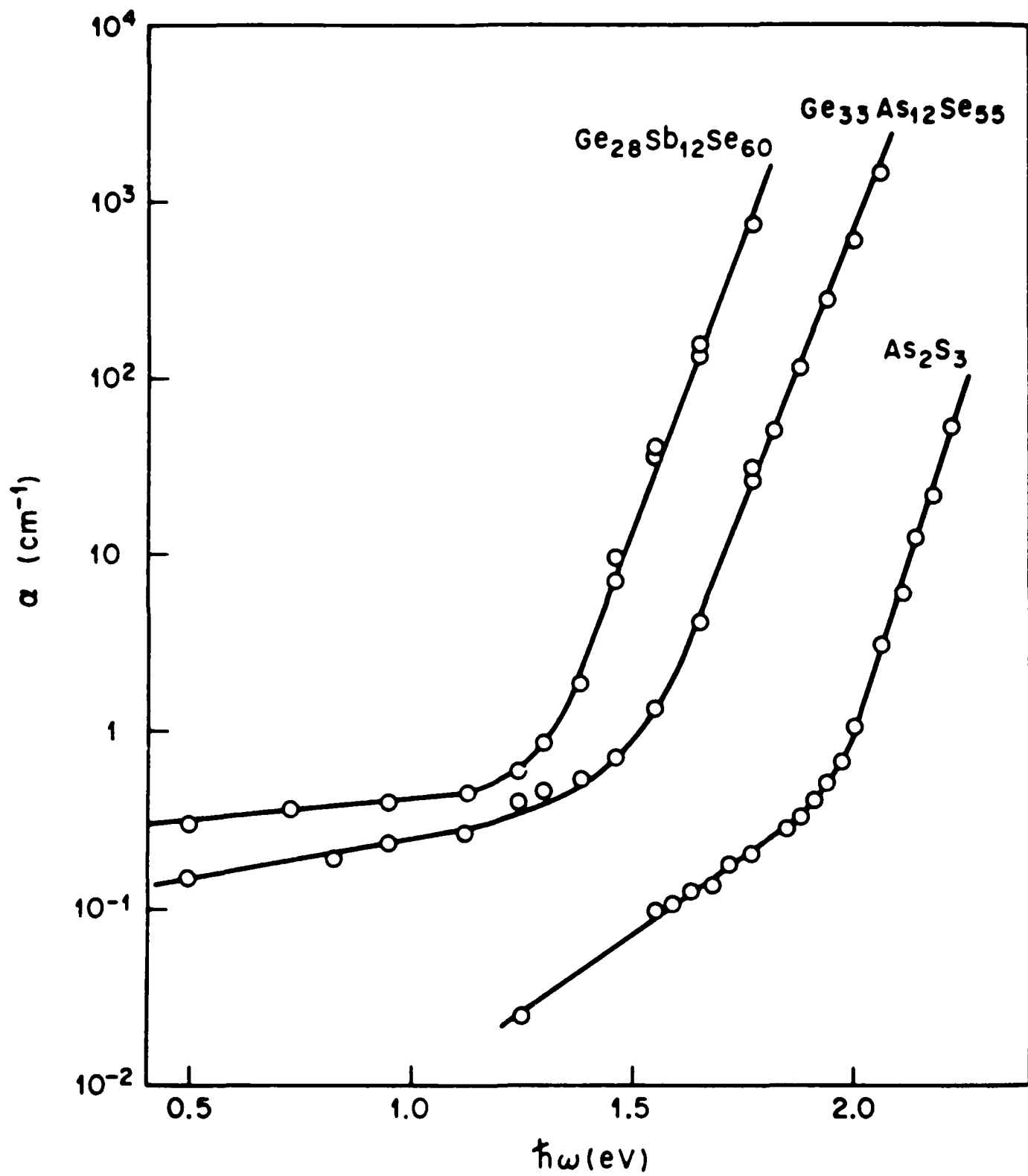


Fig. 6

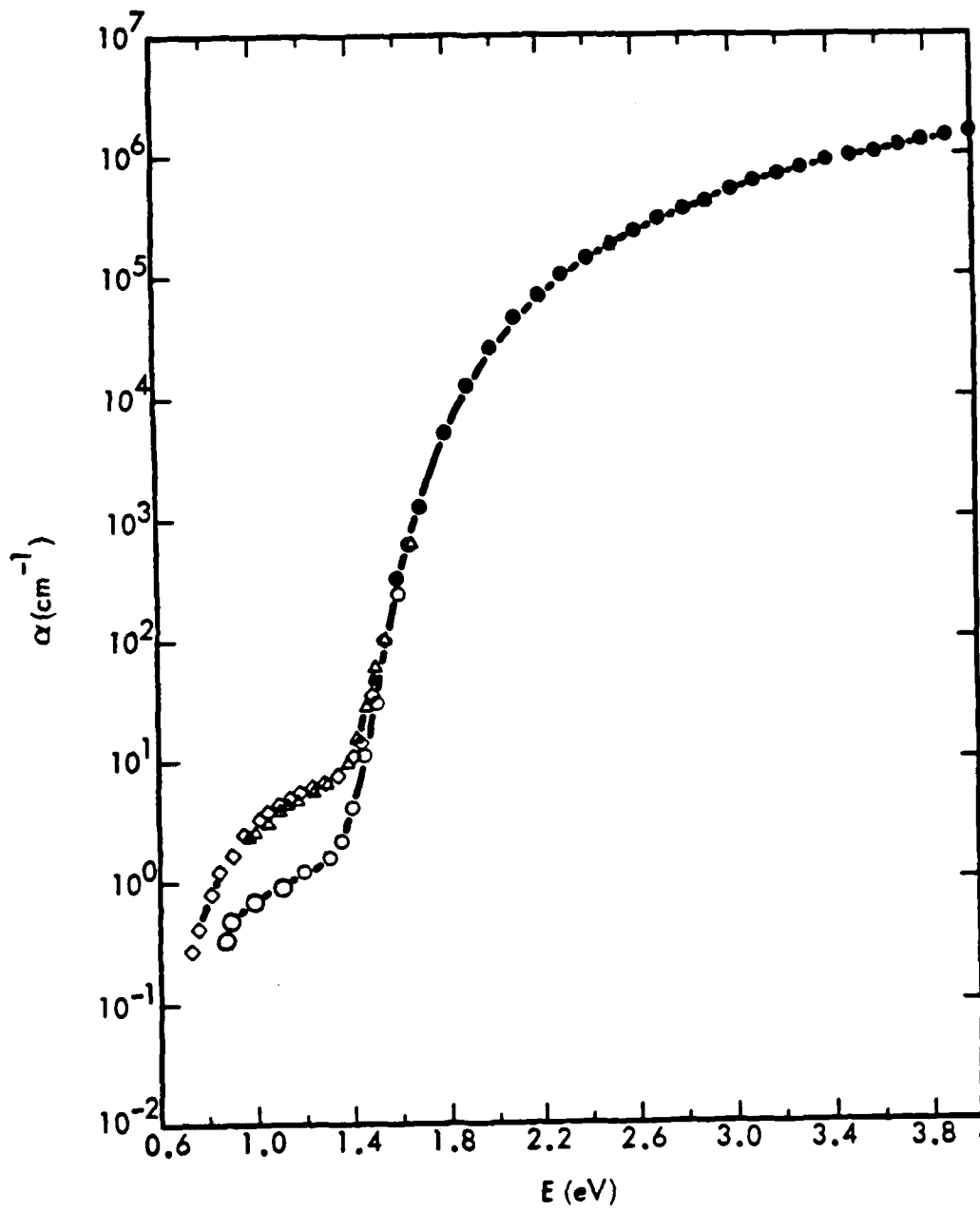


Fig. 5

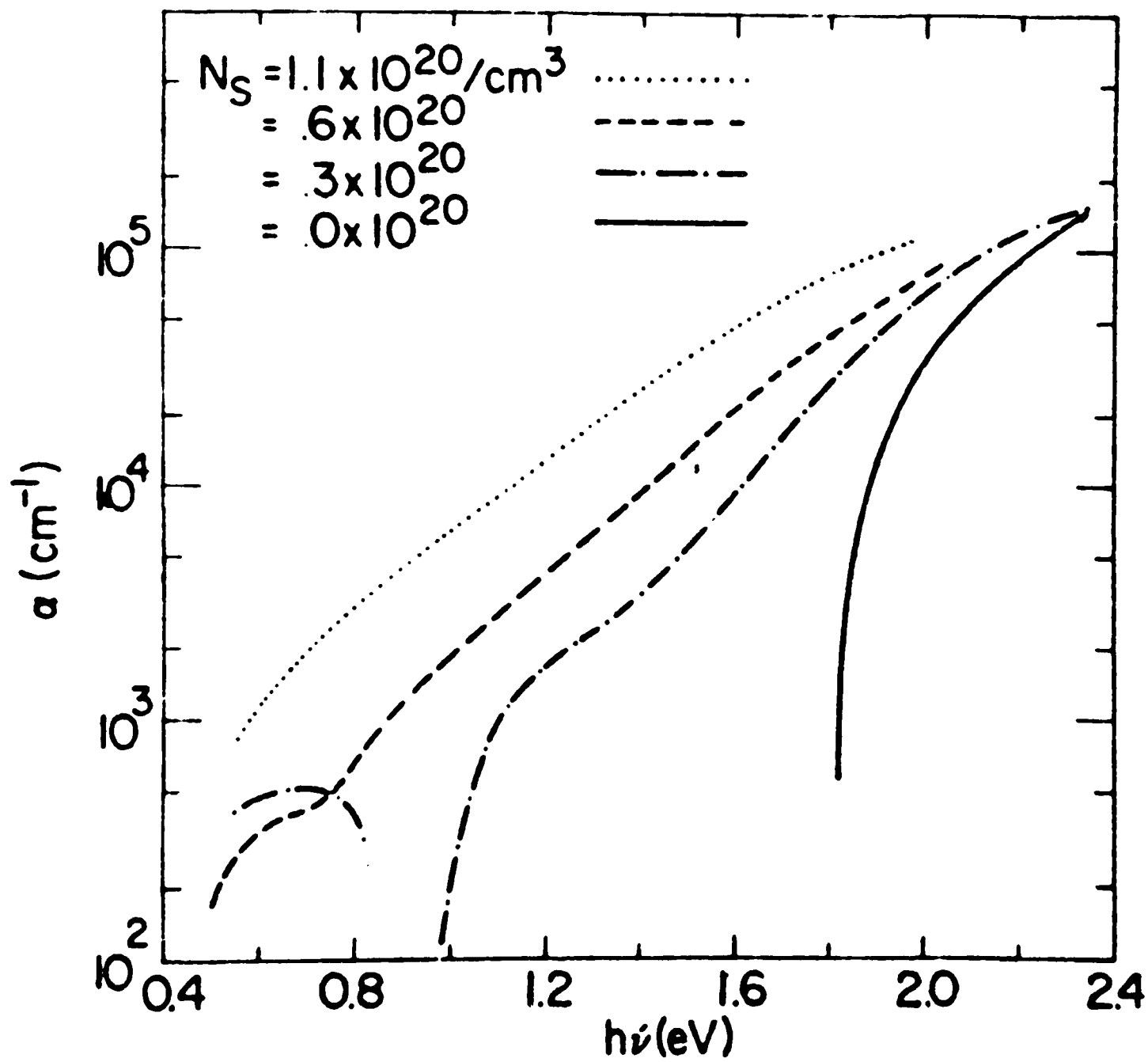


Fig. 4



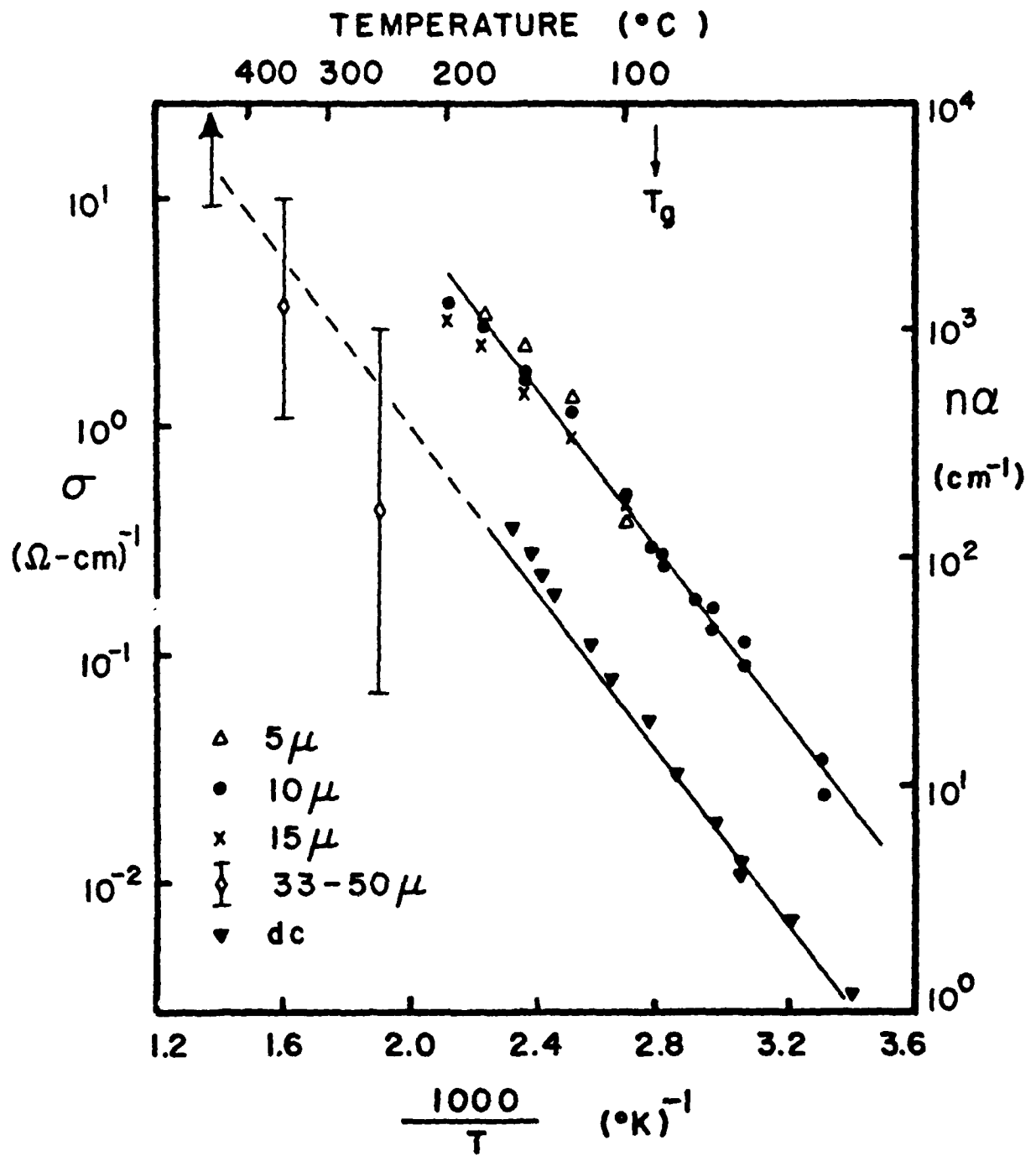


Fig. 17

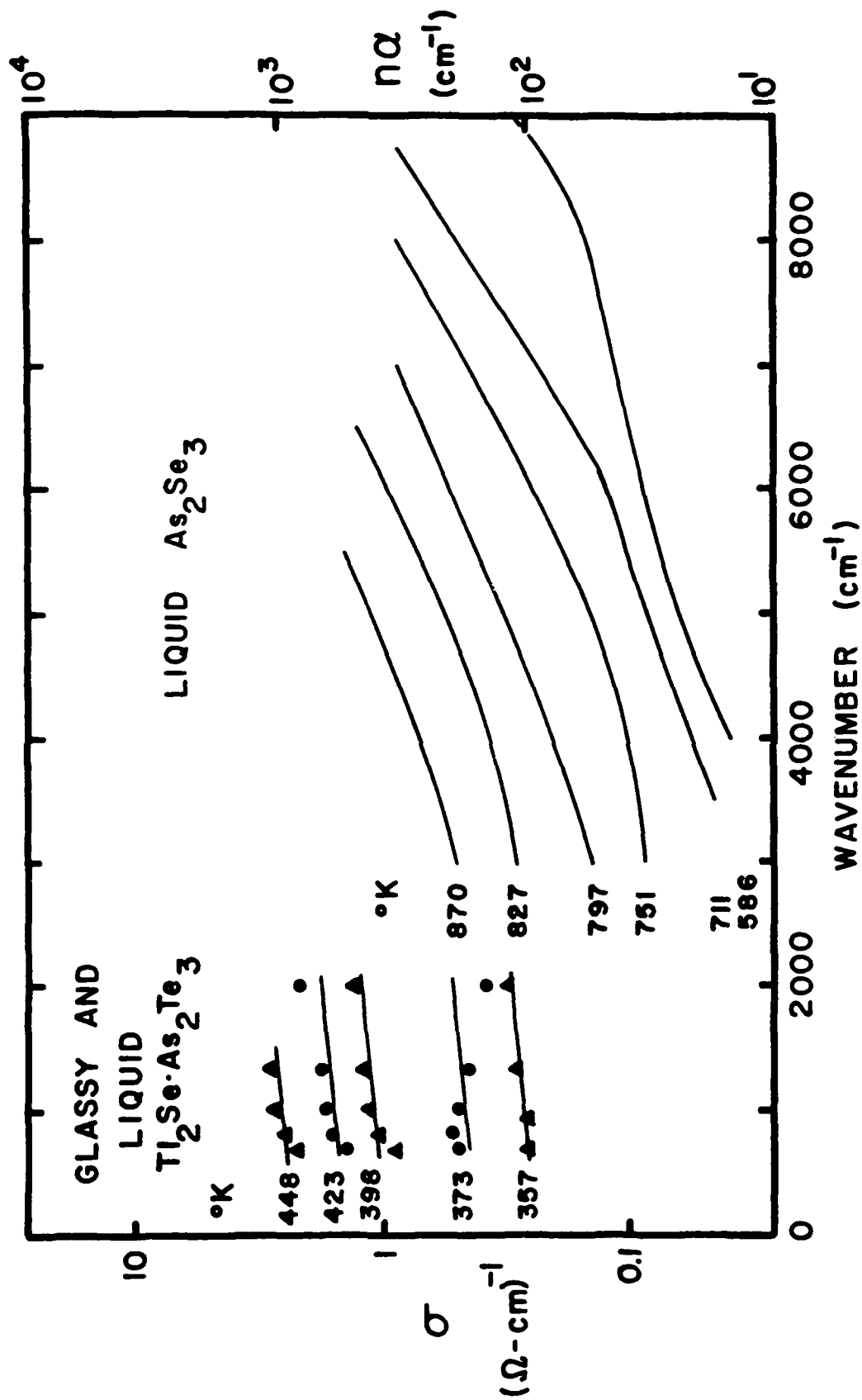


Fig. 18

**END**

**FILMED**

7-85

**DTIC**

**END**

**FILMED**

7-85

**DTIC**